

# Team Results Document

# MakeSense



上海科技大学  
ShanghaiTech University



MakeSense  
ShanghaiTech



SensUs 2025 Acute Kidney Injury

ShanghaiTech University

## TEAM MEMBERS

### Captain

Terry Wang  
Rong Shao

### Wet Lab

Yuchen Hao  
Chen Liu  
Wanxiang Xiong

### Dry Lab

Kaizhan Lin  
Chuhe Wen  
Qihang Yan  
Haotian Zhu  
Jingting Zhang  
Wenye Xiong

### Translation

Runlin Dong  
Linjia Liu

### SUPERVISOR

Ze Xiong  
Suwen Zhao  
Daniel Koo

### COACHES

Jiayi Liu  
Feifan Liu



8-8-2025

## 1. Abstract

We developed a modular creatinine biosensor system based on a three-enzyme cascade with replaceable electrode design. Initially, we designed microneedle-based interstitial fluid (ISF) sensor modules targeting high-frequency monitoring needs of acute kidney injury (AKI) patients. However, research revealed creatinine monitoring equally benefits chronic kidney disease (CKD) patients and health-conscious individuals, though their monitoring requirements do not require continuous invasive detection. Therefore, we expanded the technology to non-invasive sweat-based detection by incorporating sweat microfluidic electrode modules into the replaceable electrode system.

During the development process, we introduced several technical innovations: innovatively employing upstream cascade enzymes to construct protective layers, effectively eliminating interference from creatine and sarcosine; developing a coin-sized wireless electrochemical platform achieving 1.74 nA detection resolution with excellent linearity ( $R^2 > 0.99$ ); the modular architecture enables long-term reuse of electronic modules—users only need to replace electrode modules, significantly reducing costs. Through our mobile application, users can monitor creatinine concentrations and glomerular filtration rate in real-time, receiving personalized health reports. This innovative platform provides customized kidney function monitoring solutions for individuals across different health states.

## 2. AP award

### 2.1. Molecular recognition

We utilized a three-enzyme cascade system comprising creatininase, creatinase, and sarcosine oxidase to convert creatinine into detectable hydrogen peroxide. The biosensor adopts a multilayer architecture in which the enzyme working layer uses trehalose and Triton X-100 to maintain enzyme structural stability and activity, with glutaraldehyde-BSA crosslinking for enzyme immobilization (Liu et al., 2022). The blocking layer contains specific cascade enzymes to consume interfering intermediates in the physiological environment (Lopez et al., 2017). Nafion incorporated between layers regulates substrate diffusion and minimizes interference (Yang et al., 2025). The PVA-PEG hydrogel encapsulation layer provides protection and enables biofluid collection (Liu et al., 2022; Promphet et al., 2025). This design enables highly specific, stable, and rapid detection of creatinine.

### 2.2. Physical transduction

We employ Prussian blue (PB)—an artificial peroxidase—as the electron mediator to monitor  $\text{H}_2\text{O}_2$  reduction. PB is mixed with graphite ink and screen-printed as working electrodes. At -0.1 V, PB is reduced to Prussian white (PW) and subsequently reoxidized to PB by  $\text{H}_2\text{O}_2$ , forming a PB/PW redox cycle (Karyakin et al., 1999; Ricci & Paleschi, 2005).

$\text{H}_2\text{O}_2$  concentration is proportional to the generated current, enabling efficient signal conversion. The low operating potential of PB significantly suppresses interferents such as ascorbic acid, enhancing detection selectivity (Liu et al., 2022).

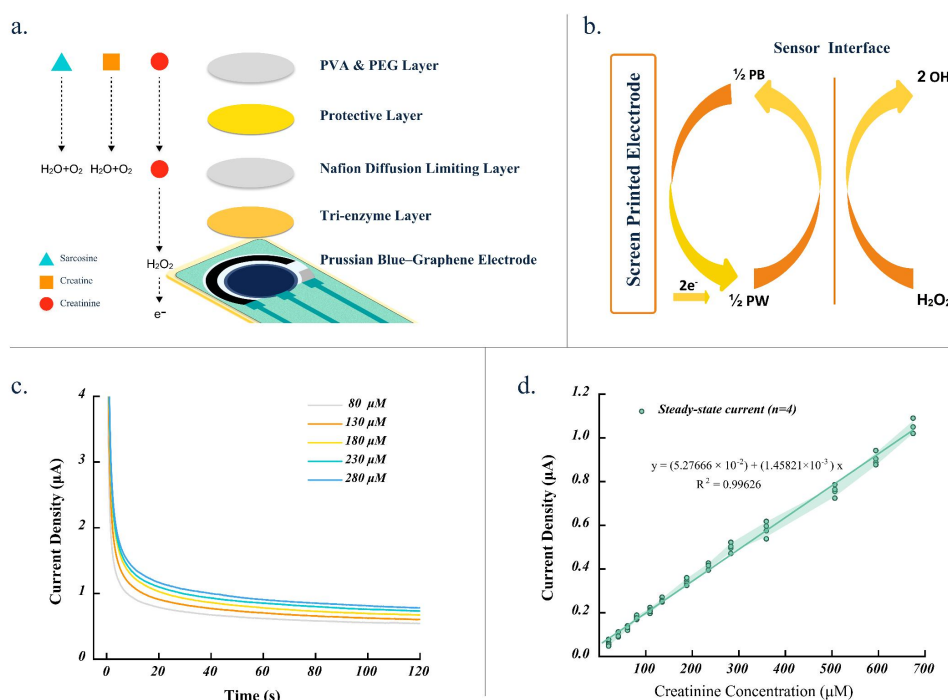


**Figure 1.** (a) Schematic of the multilayer biosensor architecture, including enzyme layer, diffusion limiting layer, and protective layers. (b) Electron transfer mechanism based on the redox cycle of Prussian Blue and hydrogen peroxide. (c)  $I$ - $T$  responses under different creatinine concentrations. (d) Calibration curve showing the linear relationship between creatinine concentration and current response.

### 2.3. Cartridge technology

We designed a 40  $\mu L$  volume microfluidic reaction chamber based on the electrode structure. Compared to traditional circular chambers, it features large-radius curves, shortened transition channels, and chamfered corners to reduce boundary layer separation and backflow, improving stability and controllability (Fu et al., 2024).

The system includes a sample reservoir, tubing, and micropump. During operation, 40  $\mu L$  of liquid is initially withdrawn into the reaction chamber at 100  $\mu L/min$  for detection. After measurement, a three-stage replacement procedure is performed at 100  $\mu L/min$ . The first stage extracts the entire 40  $\mu L$  post-reaction solution, the second stage extracts 40  $\mu L$  of fresh solution for rinsing, and the third stage extracts 40  $\mu L$  of fresh solution for the next cycle. This process repeats continuously, enabling continuous sensing with minimal cross-contamination between samples.

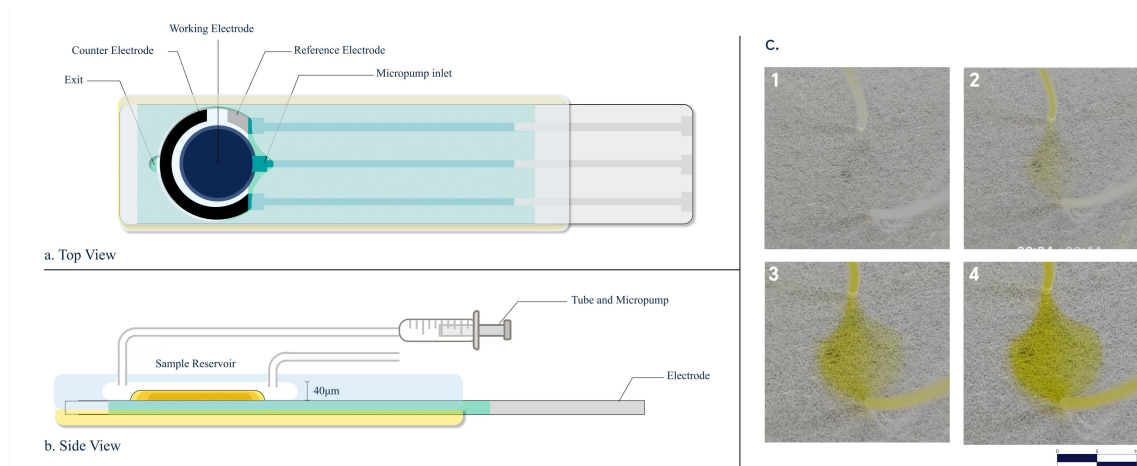


**Figure 2.** (a) Top view of the microfluidic reaction chamber integrated with electrodes and micropump inlet. (b) Side view of the syringe-driven system used for solution injection and replacement. (c) Microfluidic liquid replacement process.

## 2.4. Reader instrument and user interaction

We developed a coin-sized electrochemical platform for high-precision wearable sensing applications, with a workstation version for ETE detection. Centered around Texas Instruments' LMP91000 three-electrode AFE, it achieves 1.74 nA detection resolution and excellent linearity ( $R^2 > 0.99$ ), with wireless data transmission enabling mobile data reception.

In the future, users simply wear and activate factory-calibrated sensors. The system offers multiple monitoring modes: high-frequency for AKI patients, moderate-frequency for CKD patients, and sweat monitoring for blood creatinine calculation. Each mode provides health analysis, reports, and alerts. We are developing a workstation version addressing traditional equipment limitations.

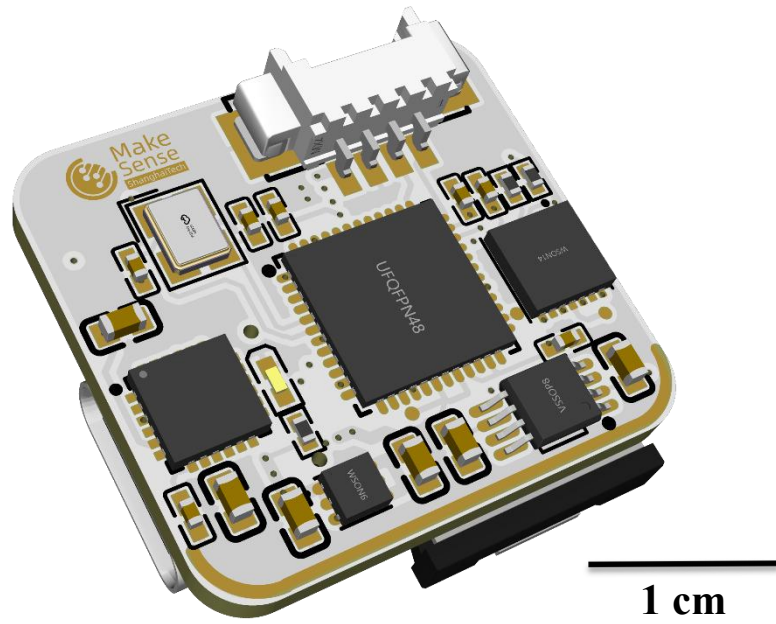


**Figure 3.** Rendered image of the custom-designed printed circuit board (PCB) for the biosensor system



### 3. IN award

#### 3.1. Wearable sensor

Acute kidney injury (AKI) monitoring requires high-frequency renal function sampling; however, existing methods rely on urine or blood samples, making real-time measurement challenging and limiting application scenarios. Based on continuous glucose monitoring (CGM) technology principles, we first developed a microneedle-based interstitial fluid creatinine sensor system that achieves enzymatic in-situ creatinine concentration monitoring through microneedles. Given that creatinine monitoring is equally applicable to chronic kidney disease (CKD) patients and healthy individuals with health monitoring needs, we recognized that the health status of these populations does not require prolonged invasive monitoring approaches. Accordingly, we constructed a sweat-based non-invasive creatinine monitoring system that employs a microfluidic platform for sweat collection and achieves creatinine concentration detection through integrated electrodes. Based on the aforementioned technical approaches, we achieved comprehensive renal function monitoring across all physiological states, encompassing acute kidney injury, chronic kidney disease, and healthy individuals, providing comprehensive renal function monitoring solutions for individuals with different health conditions.

##### 3.1.1. Technological novelty of wearable sensor

We developed a universal wearable electrochemical system with a replaceable electrode design that is compatible with electrodes for monitoring different samples such as ISF and sweat. Users only need to replace the electrode components each time, while the electronic module requires no replacement and can be reused long-term, thereby significantly reducing user costs and enhancing convenience.

We use a single-use flexible microneedle (Choi et al., 2017; Fu et al., 2024; Gao et al., 2023; Mugo et al., 2022). The flexible microneedle makes direct contact with interstitial fluid, delivering rapid response, continuous monitoring, and long-term wear. The flexible microneedle is about 5 mm long and less than 0.3 mm in diameter. Its tip is modified with a three-electrode system (working, reference, and counter electrodes) coated with a triple-enzyme cascade layer, and its tail connects via contact points to a reusable signal-processing module.

For sweat sensing, we developed a sweat microfluidic sampling system. For the single-channel sweat microfluidic sampling system, in addition to using the sweat gland itself as a pressure source, optimized capillary force and evaporative pump are also introduced to

activate sweat flow, ensuring the temporal resolution and accuracy of detection. After passing through the detection zone, creatinine in the sweat diffuses to the sensing electrode and undergoes a three-enzyme cascade reaction. After detection, the hydrophilic porous material loaded in the outlet zone further induces liquid discharge. However, sweat analysis need not be confined to creatinine. Sweat naturally contains nanoliter-scale ultrafiltrates of plasma that concurrently carry glucose, sodium, potassium, urea, cortisol, and a spectrum of inflammatory cytokines—all tightly linked to metabolic homeostasis. In 2018, the WHO's REASSURED (GADx-Team, 2024) criteria introduced the concept of multiplexed (multi-analyte) assays, mandating that a single platform simultaneously detect multiple pathogens, biomarkers, or disease-relevant indicators. Building on this, we have expanded our microfluidic sweat-sampling system by integrating a plurality of repeating units, each equipped with electrodes tailored to a target-specific sensing electrode. These collection units are arranged in parallel to ensure that the spatial orientation of multiple sensors in real scenarios is similar and to avoid interference from gravity factors during monitoring. Combined with detection electrodes capable of detecting different biomarkers, the reacted liquid flows into the combined outlet area. In addition, check capillary bursting valves are set up before the outlet area to prevent cross-contamination between compartmentstion electrodes for different biomarkers, reacted fluid flows into a combined waste zone.

Traditional enzyme-electrochemical sensing requires a bulky workstation, but wearable sensors demand strict size constraints. We developed a coin-sized platform integrating the core detection unit and Bluetooth (Hoilett et al., 2020). Using a sleep-dominated mode (3–6 measurements/hour), total power consumption is greatly reduced for long-term continuous monitoring. A 6-layer HDI PCB achieves extreme miniaturization while.

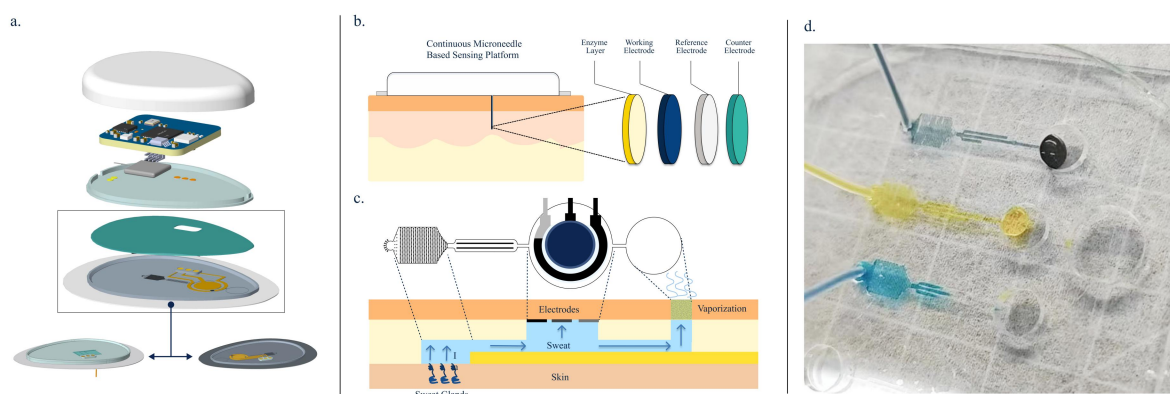


**Figure 4.** (a) Exploded view of the modular wearable sensing device with replaceable electrode and reusable PCB module. (b) Schematic of modular sensing system for ISF creatinine detection. (c) Schematic



*of modular sensing system for sweat creatinine detection. (d) Microfluidic sweat sampling device demonstration.*

preserving signal integrity and performance. We mitigate noise through hardware (low-drift precision voltage reference, RC filters at key nodes — transimpedance amplifier, analog output) and software (ADC oversampling, exponential moving average filtering). This co-design balances measurement accuracy and operational efficiency. The signal-processing module (the base) connects to sampling modules; in multi-channel setups, a sequential detection mode is planned.

### 3.1.2. Technical feasibility of wearable sensor

For the single-channel sweat microfluidic system, we built a prototype on a glass substrate and used a micro-syringe pump to inject the test solution at 100  $\mu\text{L}/\text{min}$ . Upon injecting 70  $\mu\text{L}$ , the electrode was fully wetted and excess liquid flowed into the waste zone without retention or overflow (**Fig. 4(c)**), ensuring real-time monitoring of fresh sweat.

## 3.2. Reliability of sensor output

Interstitial fluid contains interfering species, the most conspicuous of which are creatine and sarcosine—both participate in the same enzymatic cascade. We therefore introduced a sacrificial blocking layer upstream of our three-enzyme stack so that creatine and sarcosine are eliminated before they can reach the underlying creatinine-sensing triad, eliminating their contribution to the signal. This cascade-based anti-interference strategy is readily generalizable to other assays, shielding the readout from endogenous reaction intermediates. In addition, strong reductants such as ascorbate are present; we exploit Prussian Blue to catalyze  $\text{H}_2\text{O}_2$  reduction at a low potential, thereby separating this reaction from oxidations that require higher potentials and thus nullifying ascorbate interference. To further reduce matrix effects, we elect the relatively clean matrix of sweat as the analytical fluid and construct a sweat-to-interstitial-fluid inference model. Through these designs, we secure both the reliability of our in-house electrochemical platform and the precision of creatinine quantification in the concentration range of several to tens of micromolar.

### 3.2.1. Technological novelty of reliability concept

Protective Layer: To block creatine and sarcosine in interstitial fluid, we added a protective layer of creatinase (Kwon, 2012) and sarcosine oxidase outside the three-enzyme cascade. A Nafion layer (Yusoff et al., 2017) of appropriate concentration and volume separates the

two enzyme layers, ensuring target creatinine reaches the underlying enzymes and that  $\text{H}_2\text{O}_2$  produced by interferents in the blocking layer does not disturb creatinine detection. Upon contact with the electrode, the protective layer — comprising creatinase and sarcosine oxidase—first converts creatine and sarcosine to hydrogen peroxide ( $\text{H}_2\text{O}_2$ ), which is immediately decomposed by catalase present in the same layer. Creatinine continues to diffuse downward. Upon encountering the Nafion membrane, the combination of cation-exchange selectivity and hydrophobic microstructure suppresses transport of specific molecules while allowing the target creatinine to reach the intact three-enzyme cascade for accurate quantification.

Recent advances in multi-compartment pharmacokinetic modeling have enabled accurate, non-invasive prediction of blood glucose and urea from sweat. For example, Yin's team systematically developed and improved a three-compartment (blood capillary – ISF – sweat gland) convection-diffusion kinetic model, combined with individualized parameter optimization and a double-loop inverse optimization strategy, to estimate blood glucose and urea concentrations from sweat measurements with high accuracy (Spearman coefficient > 0.98) (Yin, Adelaars, et al., 2025; Yin, Peri, Pelssers, Toonder, Klous, et al., 2025). They also proposed the LDRW algorithm to further reduce parameter complexity and improve computational efficiency (Yin, Peri, Pelssers, Toonder, & Mischi, 2025). These models are fundamentally based on passive diffusion and convection, described by Fick's law, Starling's principle, and Darcy's law. Since creatinine shares these passive transport mechanisms and does not undergo active cellular uptake, this modeling framework can be feasibly extended to creatinine, requiring only adjustment of relevant parameters such as diffusion coefficients. Sensitivity analysis in the original studies also demonstrated that these physical parameters are the main determinants of model performance. Furthermore, recent work by Sophie Adelaars et al. demonstrated a measurable correlation between sweat and plasma creatinine concentrations using multivariable regression (Adelaars et al., 2025). Together, these studies provide a solid theoretical basis for modeling sweat-to-plasma creatinine kinetics and non-invasive estimation using the same strategies.

**Electrochemical Platform:** (1) **Hardware:** A low-drift precision voltage reference supplies stable reference for the ADC and analog front end, suppressing temperature-induced measurement shifts. RC filters at critical analog nodes (transimpedance amplifier) attenuate high-frequency noise before digitization. (2) **Software:** ADC oversampling spreads quantization noise across frequency and, with digital filtering, improves effective resolution; subsequent exponential moving average smoothing reduces random noise.

(3) Calibration: Due to batch-to-batch variability in electrode manufacture and enzyme immobilization, the firmware includes a calibration algorithm. When a sampling module is replaced, the user inputs module-specific calibration data; the algorithm normalizes raw signals to compensate for each electrode's unique electrochemical characteristics.

### 3.2.2. Technical feasibility of reliability concept

To assess the tolerance of the Prussian blue screen-printed electrode toward common interfering species, the electrode was sequentially immersed in PBS solutions containing dopamine, ascorbic acid, uric acid, and acetaminophen (all at the same concentration), and the resulting current changes were recorded. As shown in **Figure 5b**, the electrode exhibited only minimal current responses to these interferents, demonstrating good specificity.

To assess the selective blocking layer's anti-interference performance, we measured electrodes with and without the protective layer in solutions of creatinine, creatine, and sarcosine. As shown in **Figures 5c and 5d**, in the absence of the protective layer, the current responses to creatine and sarcosine are relatively high, approaching or even exceeding that of creatinine. In contrast, on electrodes modified with the protective layer, the current responses to creatine and sarcosine are relatively low, indicating minor interference with creatinine detection. **Figure 5d** demonstrates the theoretical feasibility of using the protective layer. Nevertheless, we are still exploring modification strategies with even better protective performance.

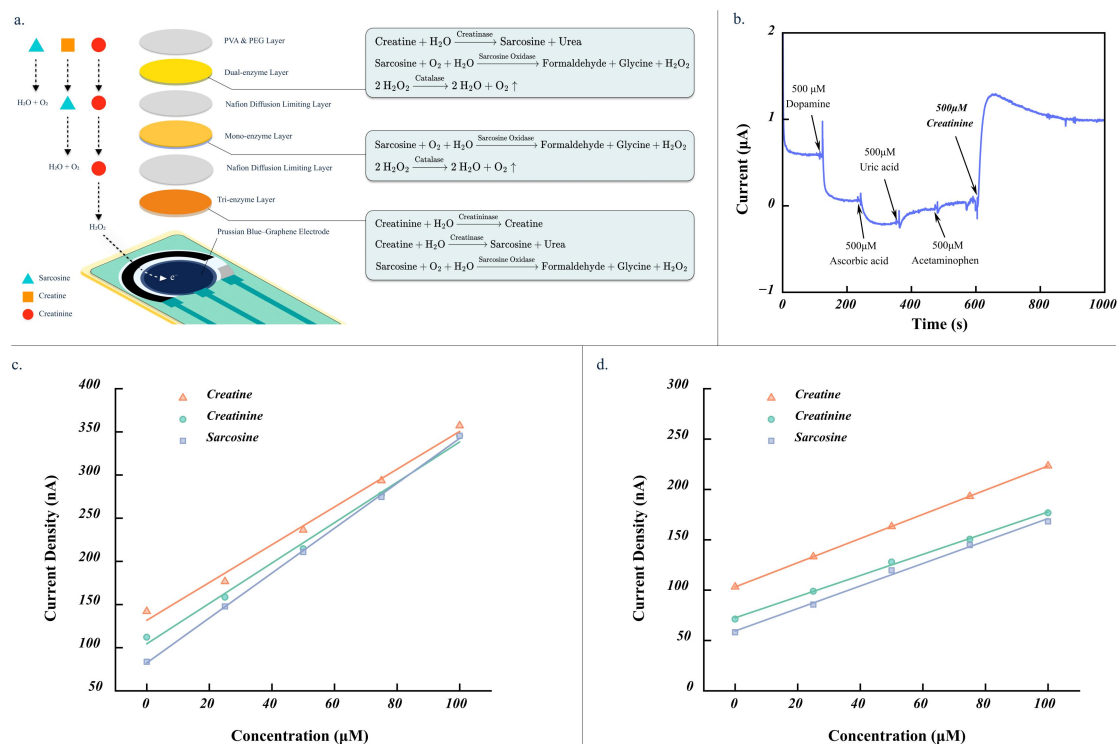


**Figure 5.** (a) Schematic of the multilayer anti-interference enzyme system. (b) Resistance evaluation of the creatinine sensor against common electroactive interferents (dopamine, ascorbic acid, uric acid, and acetaminophen). (c) The current density responses of electrodes without the protective layer to creatinine, creatine, and sarcosine. (d) The current density responses of electrodes with the protective layer to creatinine, creatine, and sarcosine.

### 3.3. Original contributions

#### Written by team captains

We evaluated different biosensing materials and platforms, then focused on electrochemical and Quartz Crystal Microbalance (QCM) approaches. Considering QCM challenges in modification, precision, and cost, we finally selected the three-enzyme electrochemical method.

For sensor interfaces, we incorporated literature methods including Prussian blue, glutaraldehyde crosslinking, Nafion, and PVA/PEG protection, while developing proprietary electrode modification strategies. Importantly, we used upstream cascade enzymes as protective layers to eliminate intermediate product interference, suppressing creatine and sarcosine interferants.

We developed a coin-sized wireless electrochemical platform with mobile application. Our modular wearable design features replaceable sensors and a proprietary sweat microfluidic system, enabling simple switching between ISF and sweat detection by changing sensor parts—enhancing convenience and reducing costs. This miniaturized wireless monitoring platform offers broad translation potential.

Novel idea conception, selection, adjustment, and testing were completed independently by our team. External contributions included reference literature, open-source projects, and advisor suggestions.

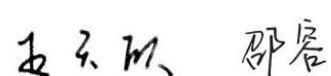
### Written by supervisors

The student team demonstrated exceptional autonomous research capabilities in developing this wearable creatinine sensor. The supervisory committee's role was limited to resource provision, directional guidance, and project evaluation.

The team independently evaluated multiple sensing platforms, selecting enzymatic electrochemical detection after identifying QCM limitations, demonstrating sound scientific judgment. Building upon existing technologies, the team achieved significant innovations: successfully optimizing Nafion/PVA-PEG protective layer formulations and creatively employing upstream enzymes to construct protective layers for interferant suppression.

The team autonomously completed hardware design, firmware programming, and application development, establishing a comprehensive wireless detection system. The sweat-based non-invasive detection scheme, from microfluidic system to concentration conversion modeling, was independently designed and implemented by students.

The developed miniaturized detection platform not only achieved project objectives but also resulted in patent acceptance for the QCM system, fully demonstrating the student team's independent thinking ability, autonomous innovation spirit, and rigorous scientific attitude.



## **4. TP award: Translation potential**

### **4.1. Customer interviews**

We grouped stakeholders into five categories: medical staff, patient-related individuals, policymakers/regulators, industrial (design & sales), and medical researchers. The first two are the primary end users; policymakers ensure compliance; and the latter two align with our team's expertise. Our target users are patients with kidney disease; once technical leadership sign-off and approvals are secured, hospitals become the direct customers. Given the intensity of contact and potential impact, we prioritized medical staff and patient-related groups, recruiting via academic and family networks to reduce barriers. Before formal interviews, we conducted desk research and pre-interviews on creatinine-related kidney diseases to refine the context, issues, and interview guides. Participants included nephrologists and nurses at tertiary hospitals, patients and their families, and policy/regulatory authorities. All sessions followed a 3:1 format—one person led the interview, one provided follow-ups, and one took notes—and we scheduled 30–60 minutes to accommodate different communication styles. With consented note-taking and rapport-building at the close, we secured authentic first-hand data to inform design and positioning.

#### **4.1.1. Interview Methods and Strategies**

We ran in-depth semi-structured interviews; question design focused on lived CKD challenges, workflow pain points, and expectations for new monitoring (2–3 core prompts plus flexible follow-ups); the total time for delivering the prepared core questions did not exceed 3 minutes, with retrospective wrap-ups; for communication and culture, we placed calls using local-IP phone numbers and used corresponding dialects for some farmers and workers to reduce wariness and exclusion.



Interviewee	Number of People	Interview Strategy	Core Question 1	Core Question 2	Core Question 3	Follow-up Question 1
Patients & Families	5 + 4	The Mom Test, situational questions, projective/third-person techniques	Have you ever experienced delayed or inaccurate testing that affected treatment?	If there was a new technology/device to monitor your health more promptly or conveniently, would you consider using it? In terms of accuracy, comfort, cost, or maintenance frequency, what matters most to you?	Among fellow patients and families, is there anything memorable you've seen... (especially about blood draws for creatinine)?	Do you think current methods for monitoring kidney function (e.g., creatinine) and providing daily care are convenient and effective? What are the main difficulties or inconveniences you face?
Doctors	8	The Mom Test, situational questions, starting from current environment	Creatinine is usually tested in routine labs for diagnosis—are there specific situations or diseases where creatinine should be monitored more closely?	How long does the full testing process take? Could creatinine change significantly during the process, making results less meaningful?	Like CGM helps track blood glucose trends for diagnosis, if we built a system for continuous creatinine monitoring, would such data help in diagnosis?	If continuous creatinine (kidney function) data were available, could it potentially become a new diagnostic standard?
Nephrology Nurses	8	Same as above	In many high-risk situations, doctors and nurses must watch patients 24/7, which is exhausting. As the primary caregivers for kidney patients, how often do high-risk situations occur compared to other diseases?	In daily care, have you encountered difficulties using or operating monitoring devices, sensors, etc.? How do these issues affect the efficiency and quality of care?	Have you noticed changes in patients' emotions during biochemical testing? If so, how does this affect nursing care?	
Medical Device Authority	2	Critical thinking, projective/third-person techniques	Have you encountered impressive student medical device development teams in your career? What were their key traits?	What is the approval timeline and prerequisites for our technology?	How could our product gain support from the Shanghai Medical Products Administration?	
Research Experts	2	Critical thinking, projective/third-person techniques	If there were a new sensor or technology for earlier, more frequent, or more convenient kidney function testing, what changes could it bring to clinical practice? What challenges might arise in adoption?	Could more timely and continuous kidney function monitoring data significantly improve clinical decisions and patient outcomes? In treatment planning, where would such data be most valuable?	If continuous creatinine (kidney function) data were available, could it potentially become a new diagnostic standard?	

#### 4.1.2. Interview Content and Reflections

We clarified core sensor functions, users, and scenarios: early misdiagnosis as gout and cost-driven delays highlight early-diagnosis gaps; a young patient noted that 1–2 months earlier detection would have improved outcomes and an acute attack progressed to dialysis, underscoring timely monitoring and alerts; a physician emphasized “creatinine is central; from CKD stage 3 onward, track decline and dialysis timing,” recommending long-term monitoring plus electrolytes (e.g., potassium, calcium) since creatinine alone is insufficient.

#### 4.1.3. Core pain points and needs in CKD management

Low early screening and high delays (CKD prevalence ~10.8%, awareness ~12.5%) demand more accessible early monitoring; infrequent, discontinuous data (monthly/quarterly tests with travel/cost barriers) raise AKI risk; patient burden and anxiety from phlebotomy and waiting for results call for real-time visibility; clinicians from stage 3 want continuous creatinine trends plus key electrolytes with EHR integration and clinical/AI support; cost and integration require affordability/reimbursement and hygienic, easy-to-use devices with replaceable/recyclable parts.

#### 4.1.4. Summary

Priorities: timelier AKI indicators, earlier deterioration monitoring for later-stage CKD, continuous multi-indicator data for decision-making, and cost-controlled system integration—anchored in China’s CKD/AKI landscape.

### 4.2. Design of validation study

Concept: a non-invasive, sweat-based wearable tracking creatinine + related biomarkers, linked to mobile app + cloud for home self-monitoring and hospital supervision → early warning & timely intervention. Rationale: non-invasive approaches have limited clinical substitutability, but lower barriers and psychological load improve acceptance and market potential (in appendix). Validation plan: three sequential methods—co-created journey mapping, scenario-based prototyping, function-card prioritization—to test feasibility/effectiveness and guide iteration.

#### 4.2.1. Co-Created Patient Journey Mapping

We ran a ~2-hour online workshop with one CKD-3 patient, one dialysis caregiver, and one nephrology nurse, using a shared whiteboard/sticky notes to map screening → diagnosis → routine follow-up → progression → dialysis, attach emotions/pain points, and locate real-time monitoring stages and high-impact touchpoints. Outputs highlighted health education + community screening for early stages, daily at-home creatinine with alerts as the optimal entry during CKD-4 follow-up, and insertion of a “pre-alert + follow-up visit” node before deterioration to close gaps.

#### 4.2.2. Scenario-Based Prototyping

While our creatinine CGM is in development, we simulated with CGMs—Yuwell Anytime 4 Pro and SiBionics—worn by two team members (designer, engineer) for ~2 weeks/device (May–June); a low-fi app displayed daily values, trends, and threshold alerts. Scripted events included Day-3 “+15% vs yesterday—arrange confirmatory test” and Day-7 red alert “contact your doctor immediately,” mirroring a CKD-3 patient's first week at home. Findings: continuity reduced uncertainty/anxiety, red alerts triggered action, and versus monthly testing, daily continuity surfaced anomalies ~3 weeks earlier; improvement targets are wear comfort/placement and backend filtering/aggregation with concise trend reports; at scale, data load on clinicians must be managed. If even 10% of early-stage patients act earlier, AKI-related admissions could decrease—an assumption requiring large-scale clinical validation.

#### 4.2.3. Function Card Sorting

Rationale: quantify what to build first and avoid low-priority investment; implementation: two cohorts—5 CKD patients and 3 nephrologists; findings: patients' top-3 = continuous creatinine, abnormal alerts, comfort; clinicians' top-3 = expanded parameters (esp. potassium), doctor platform, cloud analytics; other: battery life medium priority (weekly charging acceptable), cost/insurance medium–high, glucose/AI assistants lower;

implications: build continuous creatinine plus key electrolytes, timely alerts, and a doctor-facing platform first; optimize comfort and hospital integration; defer secondaries.

#### 4.2.4. Conclusion

Conclusion. The journey → scenario → cards sequence establishes a user-evidence chain from needs to implementation, supporting a wearable creatinine sensor that enables early, continuous, multi-parameter monitoring, seamless clinical integration, and reduced care burden; development priorities center on electrolyte inclusion (e.g., potassium), alert accuracy, clinician-usable summaries, and cost/reimbursement alignment. In parallel, this work prepares productization research before compliance testing for our current invasive, body-fluid-based creatinine sensor, and builds methodological experience for a future sweat-based, non-invasive sensor.

## 5. Team and support

### 5.1. Contributions of the team members

**Terry Wang:** Served as project captain and led sensor interface modification strategy development. Conducted wet laboratory experiments and contributed to translation and commercialization.

**Rong Shao:** Co-captain responsible for sensor interface modification strategy development and wet laboratory experiments.

**Kaizhan Lin:** Core developer of the coin-sized electrochemical platform and architect of the QCM sensing system.

**Chuhe Wen:** Designed and implemented the microfluidic system for sample handling and processing.

**Yuchen Hao:** Conducted wet laboratory experiments and contributed to sensor interface modification strategy development.

**Chen Liu:** Performed wet laboratory work focusing on sensor interface modification strategy development and contributed to translation and commercialization.

**Wanxiang Xiong:** Performed wet laboratory work focusing on sensor interface modification strategy development and contributed to translation and commercialization.

**Jingting Zhang:** Developed hardware components and participated in electrochemical platform engineering.

**Mason Dong:** Lead designer responsible for sensor structural design and commercial translation strategy.

**Linjia Liu:** Developed software solutions for data acquisition and analysis systems.

**Haotian Zhu:** Developed algorithms for sweat-based biomarker analysis and data processing.

**Qihang Yan:** Contributed to hardware development and system integration.

**Wenye Xiong:** Founded the instrumentation development division.

### 5.2. People who have given support

**Feifan Liu:** Provide help during hardware survey.

**Dan Li:** Provide suggestion for hardware solutions and support for hardware resources.

**Jiayi Liu:** Provide suggestion for wetlab design and experiments.

**Jing Yang:** Provide support for wetlab resources.

**Bohan Zhang:** Hardware advisor.

**Li Yuzhen:** Engineer, assisted in capturing SEM images of electrode samples.

### 5.3. Sponsors and partners

**PalmSens:** Conducted the Partner Session with us and provided guidance on the industrialization and commercialization of sensors.

**SUNJEEN:** Electrode Supplier.

## 6. Final remarks

Our biosensor platform has demonstrated excellent precision and linear range in laboratory settings, providing technical support for real-time monitoring of interstitial fluid and sweat. With these validated capabilities, we have expanded the application scenarios of kidney function monitoring from AKI to CKD patients and healthy individuals with health monitoring needs, and proposed corresponding monitoring solutions. Currently, our sensors have completed proof-of-principle validation and preliminary design, and are about to enter the complete industrial design and commercialization phase. We look forward to bringing this technology to market and making substantial contributions to human health.

As a team participating in this competition for the first time, we built a biosensor design and validation platform from scratch. While this process was full of challenges, it has also been extremely instructive—beyond technical breakthroughs, we conducted extensive commercialization research and user interviews, gaining deep insights into the project's translational potential and practical significance from an empathetic perspective, which helped us understand that the goal of scientific research is to serve human well-being.

We would like to express our heartfelt gratitude to the School of Life Science and Technology, School of Biomedical Engineering, School of Physical Science and Technology, and School of Creativity and Art at ShanghaiTech University for their strong support.

We are looking forward to the upcoming Eindhoven Innovation Day, where we hope to engage in meaningful exchanges with exceptional teams from around the globe to drive forward the development of biosensor technology together.



## 7. References

- Adelaars, S., Lapré, C. S. M., Raaijmakers, P., Konings, C. J. A. M., Mischi, M., Bouwman, R. A., & van de Kerkhof, D. (2025). A novel LC–MS/MS assay for low concentrations of creatinine in sweat and saliva to validate biosensors for continuous monitoring of renal function. *Journal of Chromatography B*, 1252, 124444. <https://doi.org/https://doi.org/10.1016/j.jchromb.2024.124444>
- Choi, J., Kang, D., Han, S., Kim, S. B., & Rogers, J. A. (2017). Thin, Soft, Skin–Mounted Microfluidic Networks with Capillary Bursting Valves for Chrono–Sampling of Sweat. *Advanced Healthcare Materials*, 6(5), 1601355. <https://doi.org/https://doi.org/10.1002/adhm.201601355>
- Fu, X., Qiu, Y., Zhang, H., Tian, Y., Liu, A., & Wu, H. (2024). Microfluidic sweat patch based on capillary force and evaporation pump for real–time continuous sweat analysis. *Biomicrofluidics*, 18(3). <https://doi.org/10.1063/5.0208075>
- GADx–Team. (2024). REASSURED: A framework for developing diagnostics for resource limited settings. <https://www.globalaccessdx.com/reassured-a-framework-for-developing-diagnostics-for-resource-limited-settings/>
- Gao, F., Liu, C., Zhang, L., Liu, T., Wang, Z., Song, Z., Cai, H., Fang, Z., Chen, J., Wang, J., Han, M., Wang, J., Lin, K., Wang, R., Li, M., Mei, Q., Ma, X., Liang, S., Gou, G., & Xue, N. (2023). Wearable and flexible electrochemical sensors for sweat analysis: a review. *Microsystems & Nanoengineering*, 9(1), 1. <https://doi.org/10.1038/s41378-022-00443-6>
- Hoilett, O. S., Walker, J. F., Balash, B. M., Jaras, N. J., Boppana, S., & Linnes, J. C. (2020). KickStat: A Coin–Sized Potentiostat for High–Resolution Electrochemical Analysis. *Sensors*, 20(8), 2407. <https://www.mdpi.com/1424-8220/20/8/2407>
- Instruments, T. (2023). REF50xx low–noise, low–drift, high–precision voltage reference (No. SBOS410K). <https://www.ti.com/lit/ds/symlink/sbos410.pdf>
- Karyakin, A. A., Karyakina, E. E., & Gorton, L. (1999). On the mechanism of H<sub>2</sub>O<sub>2</sub> reduction at Prussian Blue modified electrodes. *Electrochemistry Communications*, 1(2), 78–82. [https://doi.org/https://doi.org/10.1016/S1388-2481\(99\)00010-7](https://doi.org/https://doi.org/10.1016/S1388-2481(99)00010-7)
- Kwon, K., & Lim, E. (2012). *Creatinine biosensors with reduced interference from creatine* (Korean Patent No. KR101163678B1). K. I. P. Office. <https://patents.google.com/patent/KR101163678B1>
- Liu, Y., Luo, X., Dong, Y., Hui, M., Xu, L., Li, H., Lv, J., Yang, L., & Cui, Y. (2022). Uric acid and creatinine biosensors with enhanced room–temperature storage stability by a multilayer enzyme matrix. *Analytica Chimica Acta*, 1227, 340264. <https://doi.org/https://doi.org/10.1016/j.aca.2022.340264>
- Lopez, F., Ma, S., Ludwig, R., Schuhmann, W., & Ruff, A. (2017). A Polymer Multilayer Based Amperometric Biosensor for the Detection of Lactose in the Presence of High

- Concentrations of Glucose. *Electroanalysis*, 29(1), 154–161. <https://doi.org/https://doi.org/10.1002/elan.201600575>
- Mugo, S. M., Dhanjai, Lu, W., & Robertson, S. (2022). A Multipurpose and Multilayered Microneedle Sensor for Redox Potential Monitoring in Diverse Food Analysis. *Biosensors*, 12(11), 1001. <https://www.mdpi.com/2079-6374/12/11/1001>
- Promphet, N., Akgönüllü, S., Moonla, C., Nandhakumar, P., Tanglertsampan, P., Laochai, T., Laichuthai, N., Wang, J., & Rodthongkum, N. (2025). Non-invasive fingertip sweat biosensor for early kidney disease biomarker screening. *Sensors and Actuators B: Chemical*, 441, 137967. <https://doi.org/https://doi.org/10.1016/j.snb.2025.137967>
- Ricci, F., & Palleschi, G. (2005). Sensor and biosensor preparation, optimisation and applications of Prussian Blue modified electrodes. *Biosensors and Bioelectronics*, 21(3), 389–407. <https://doi.org/https://doi.org/10.1016/j.bios.2004.12.001>
- Yang, J., Yu, R., Zhang, W., Wang, Y., & Deng, Z. (2025). Electrochemical Determination of Creatinine Based on Multienzyme Cascade-Modified Nafion/Gold Nanoparticles/Screen-Printed Carbon Composite Biosensors. *Sensors*, 25(13), 4132. <https://www.mdpi.com/1424-8220/25/13/4132>
- Yin, X., Adelaars, S., Peri, E., Pelssers, E., Den Toonder, J., Bouwman, A., Van de Kerkhof, D., & Mischi, M. (2025). A novel kinetic model estimating the urea concentration in plasma during non-invasive sweat-based monitoring in hemodialysis [Original Research]. *Frontiers in Physiology*, Volume 16 – 2025. <https://doi.org/10.3389/fphys.2025.1547117>
- Yin, X., Peri, E., Pelssers, E., Toonder, J. d., Klous, L., Daanen, H., & Mischi, M. (2025). A personalized model and optimization strategy for estimating blood glucose concentrations from sweat measurements. *Computer Methods and Programs in Biomedicine*, 265, 108743. <https://doi.org/https://doi.org/10.1016/j.cmpb.2025.108743>
- Yin, X., Peri, E., Pelssers, E., Toonder, J. D., & Mischi, M. (2023, 14–16 June 2023). Estimation of blood glucose levels by sweat sensing based on biophysical modeling of glucose transport. *2023 IEEE International Symposium on Medical Measurements and Applications (MeMeA)*.
- Yin, X., Peri, E., Pelssers, E., Toonder, J. d., & Mischi, M. (2025). Real-time estimations of blood glucose concentrations from sweat measurements using the local density random walk model. *Medical & Biological Engineering & Computing*. <https://doi.org/10.1007/s11517-025-03393-z>
- Yusoff, N., Rameshkumar, P., Mehmood, M. S., Pandikumar, A., Lee, H. W., & Huang, N. M. (2017). Ternary nanohybrid of reduced graphene oxide-nafion@silver nanoparticles for boosting the sensor performance in non-enzymatic amperometric detection of hydrogen peroxide. *Biosensors and Bioelectronics*, 87, 1020–1028. <https://doi.org/https://doi.org/10.1016/j.bios.2016.09.045>

- Community, C. (2025). *Bluetooth-le: Bluetooth LE plugin documentation*.  
<https://github.com/capacitor-community/bluetooth-le>
- Team, I. (2025). Capacitor camera plugin & capacitor-native-settings.  
<https://capacitorjs.com/docs/apis/camera>
- Inc, A. (2025). Apple human interface guidelines. <https://developer.apple.com/design/human-interface-guidelines/>

## 8. Appendix

### 8.1. Supplementary Data on Electrode Properties

#### Electrode SEM Characterization

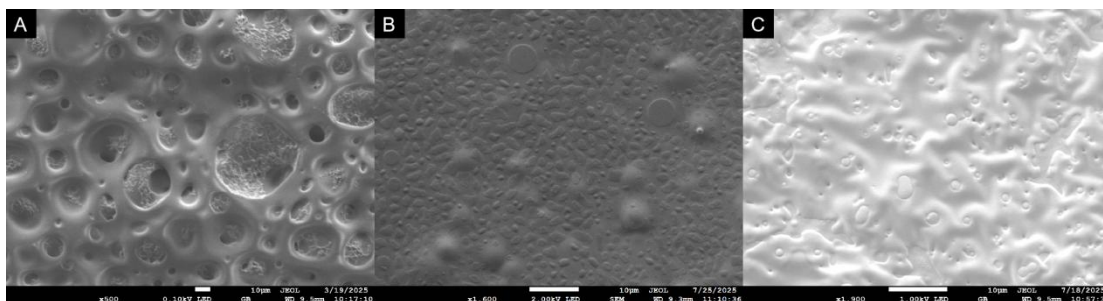


**Figure 1.** SEM characterization of surface-modified electrodes. (A) PVA/PEG composite hydrogel encapsulation. (B) Thickness-optimized PVA/PEG encapsulation with enhanced durability. (C) Poly-L-lysine (PLL) functionalized surface.

#### Electrode Performance Evaluation

The electrochemical performance of the modified electrode was evaluated by cyclic voltammetry (CV) within a potential window of -1 V to +1 V at various scan rates. The measurement results are shown in Figure 2.

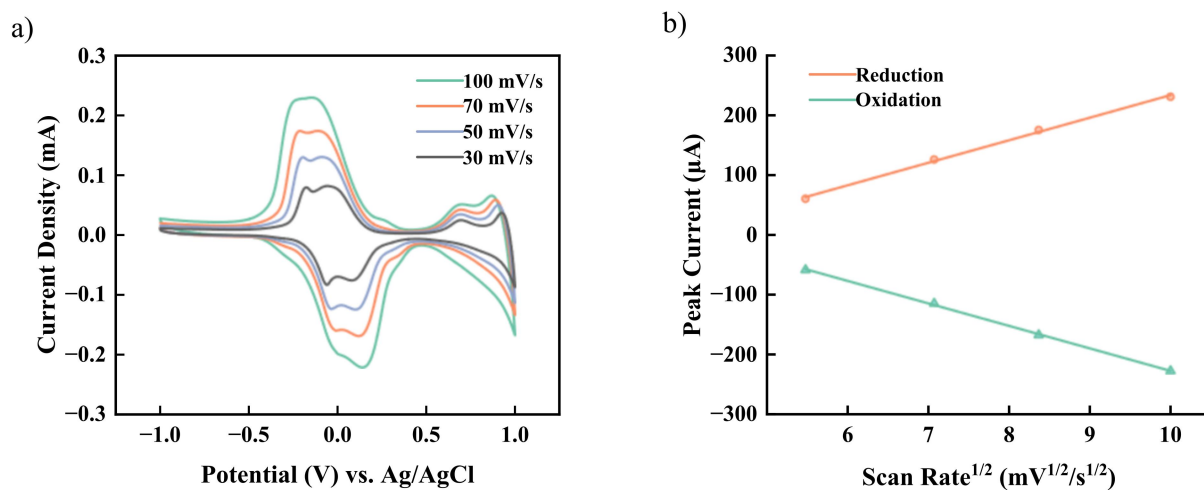


**Figure 2.** Results of cyclic voltammetry (CV) analysis. (a) CV curves at different scan rates; (b) Relationship between peak current and the square root of scan rate derived from the CV curves.

The results demonstrate that the electrode exhibits excellent CV performance (Figure 2a). Both the oxidation and reduction peak currents increase linearly with the square root of the scan rate, in accordance with the Randles-Sevcik equation, indicating a predominantly diffusion-controlled sensing process (Figure 2a, b).

## Electrode Calibration

Amperometric measurements (I-T) were performed at an applied potential of -0.1 V to record current responses at varying creatinine concentrations. The acquired data were fitted to establish the sensor's current-concentration calibration curve, with the measurement and fitting results presented in Figure 3.

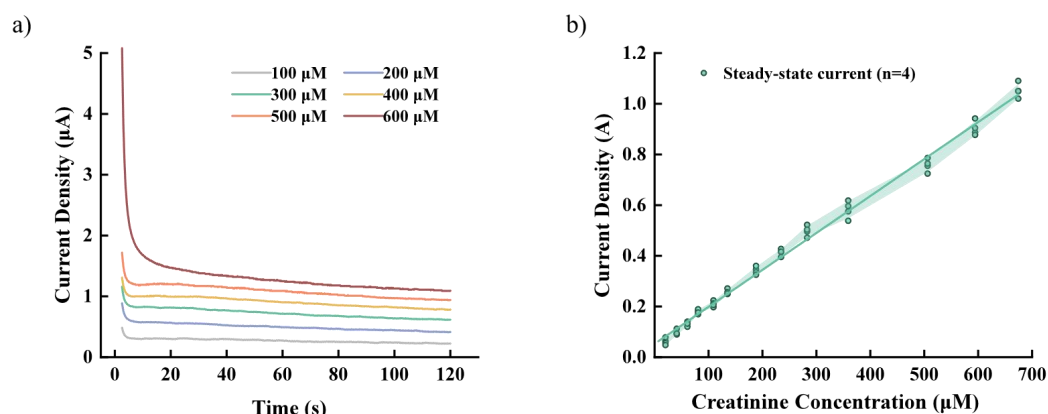


**Figure 3.** Calibration measurement results of the electrode. (a) Current-time curves at different creatinine concentrations; (b) Fitting results of the calibration curve.

The current exhibited a linear increase with rising creatinine concentrations. The sensor demonstrated a linear detection range of 30-800  $\mu\text{M}$  with a sensitivity of 1.458 nA/ $\mu\text{M}$ . Excellent linearity was confirmed by a correlation coefficient ( $r$ ) of 0.9983 and determination coefficient ( $R^2$ ) of 0.9966. The system showed remarkable precision, with single-point linearity deviation  $<\pm 20\%$  and coefficient of variation  $<\pm 3\%$  at fixed concentrations (Figure 3b). These results confirm the successful fabrication of a creatinine-sensitive electrode with practical applicability as a creatinine sensor.

## Electrode Application Testing

The modified electrode was immersed in PBS solution with varying creatinine concentrations, and amperometric measurements (I-T) were conducted at an applied potential of -0.1 V to record current responses across varying creatinine concentrations. The measured current values were interpolated using the sensor's calibration curve to determine the corresponding creatinine concentrations. As shown in Figure 4, excellent agreement was observed between the measured and actual concentrations, demonstrating the sensor's quantification accuracy.

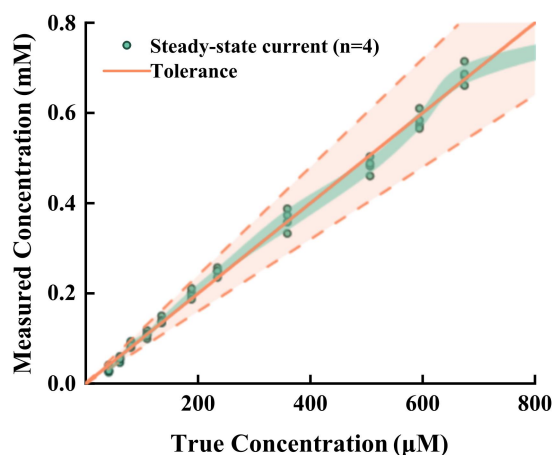


**Figure 4.** Comparison between sensor-measured concentrations and actual creatinine concentrations.

The measured concentrations consistently demonstrated less than 20% deviation from actual values, confirming the successful application of our creatinine sensor for accurate quantification of unknown samples with <20% measurement error.

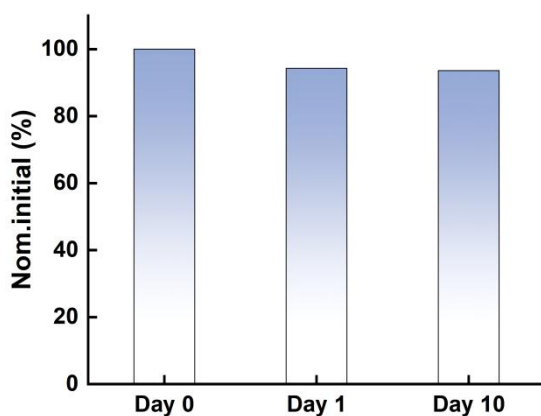


**Figure 5.** Investigation of the stability of creatinine biosensor with the detection of  $500\ \mu\text{M}$  creatinine.

The stability test of the sensor (Figure 5) showed that the electrode retained more than 93% of its initial response after being stored at room temperature for 10 days, indicating good stability of our sensor.



## Electrode Interference Testing

Many electroactive substances in the blood, such as dopamine, ascorbic acid, uric acid, etc., can affect the accuracy of the biosensor. To verify the resistance of the electrode to common interfering substances, the electrode was sequentially immersed in a PBS solution of the interfering substance and creatinine (at the same concentration) and the current change was measured. The results are shown in Figure 6.

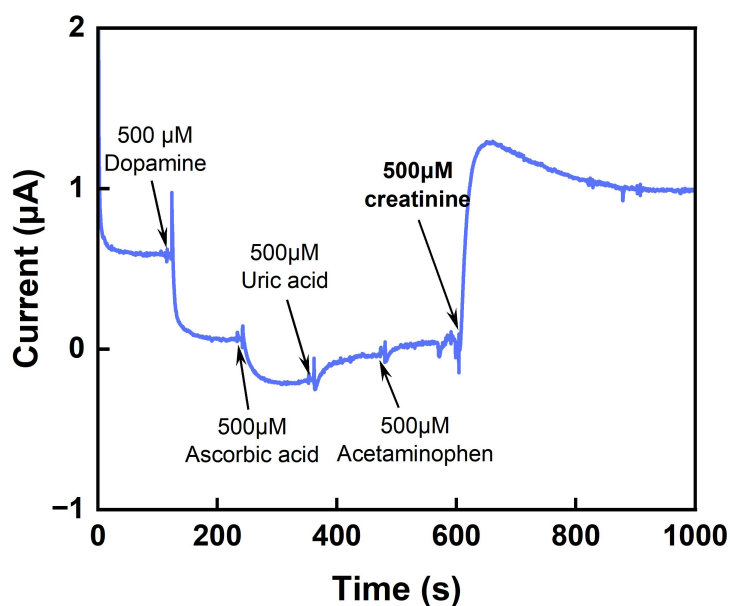


**Figure 6.** Resistance evaluation of the creatinine sensor against common electroactive interferents (dopamine, ascorbic acid, uric acid, and acetaminophen).

The results demonstrate that the current signals generated by interferents were significantly weaker than those produced by creatinine, confirming the superior selectivity of our creatinine sensor.

To evaluate the protective layer's anti-interference capability against cascade reaction intermediates, the modified electrodes with or without the protective layer were immersed in PBS solutions containing gradient concentrations of either creatinine, creatine or sarcosine. The steady-state currents were measured, and the current-concentration relationships were linearly fitted to generate calibration curves, as shown in Figure 7.

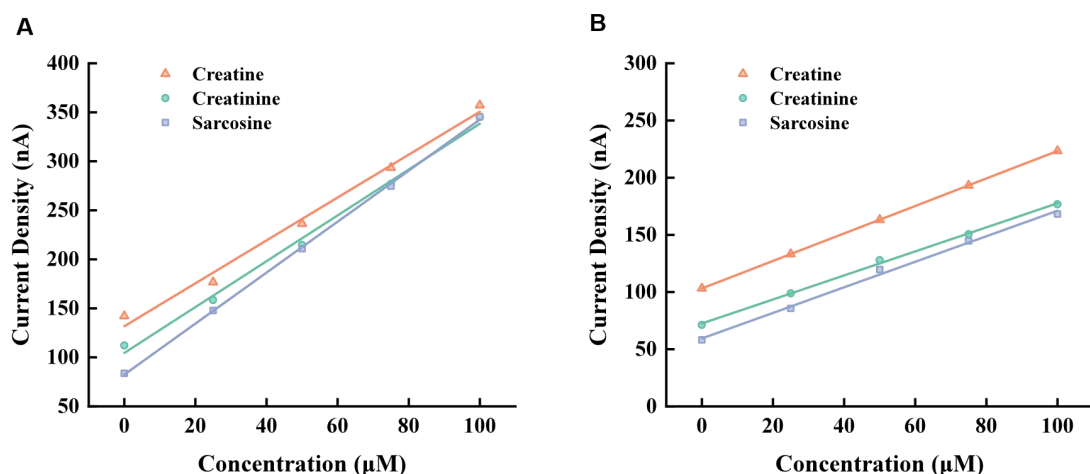


**Figure 7.** Sensor response curves for creatinine and interference (creatine, sarcosine) detection. (A) Modified electrode without the protective layer. (B) Modified electrode with the protective layer.

The bare electrode (without the protective layer) generated similar current responses when measuring creatinine, creatine, and sarcosine. In contrast, the electrode with a protective layer exhibited a higher current response toward creatinine compared to creatine and sarcosine, which confirms the sensor's anti-interference capability against cascade reaction intermediates.

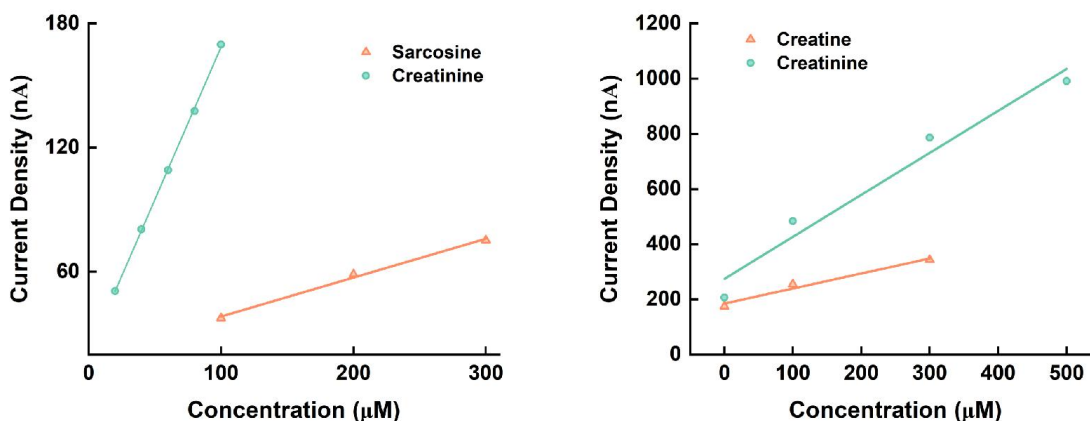


**Figure 8.** Successful case showing that the electrode exhibits significantly higher sensitivity toward creatinine compared to interferences (creatine and sarcosine).

However, the incorporation of a protective layer against intermediates significantly increases structural complexity and modification difficulty, posing challenges to electrode consistency and reproducibility. While we have obtained promising data (Figure 8) demonstrating effective shielding against intermediate interference, which highlights the design's potential, we currently face challenges in replicating these experimental results.

We are actively working to improve the reliability and effectiveness of this design to achieve enhanced performance.

## 8.2. Poly-L-Lysine Modification

### Motivation

The following problems occurred in the previously used electrode preparation scheme: 1) It could not be preserved for a long time; 2) Whether on the freshly prepared electrodes or those that have been stored for a long time, the problem of weak current signals has occurred. Some assumptions have been made about the degeneration of electrode, one possible reason is that: The use of PVA as protective layer can not hold the enzyme molecules.

PVA is a kind of linear polymer material, synthesized from polyvinyl alcohol as the monomer, exhibits potential limitations for electrode stabilization in bio-sensing applications. Their inherent linear molecular architecture affords inadequate mechanical robustness, rendering the layers prone to fracture and delamination under operational stresses. Furthermore, the open, non-crosslinked structure provides insufficient confinement for encapsulated small biomolecules, such as enzymes. This results in substantial leakage and premature desorption of the biocatalytic components, leading to rapid degradation of electrode sensitivity, stability, and functional lifespan. For the promotion, in the PVA molecule, the only reactive group is the hydroxyl group on the side chain of the monomer. However, its reactivity is weak and it is difficult to form a network structure on the electrode surface without damaging the enzyme activity.

To overcome these critical drawbacks, we introduce a robust crosslinked protective layer formed via the reaction of poly-L-lysine (PLL) with glutaraldehyde (GA). Due to the rich amino group contained in PLL, GA can cross-link these amino groups to make a covalently bonded, three-dimensional polymeric network. The key advantages of this engineered structure are twofold: Firstly, the interconnected network confers exceptional mechanical integrity, dramatically enhancing resistance to fracture and physical degradation. Secondly, and crucially, the dense, mesh-like architecture acts as a highly effective molecular barrier. This significantly mitigates leakage and immobilizes enzyme molecules within the matrix, drastically reducing their undesired desorption. Consequently, this approach maximizes the retention and operational stability of the bioactive components, leading to electrodes with superior long-term performance and reliability.

Different preparation protocol

1) Basic preparation of electrode

The enzyme follows the protocol of PVA electrode, and the only change is the use of Triton. In the preparation of PVA electrode, 0.1% Triton is used; while in the preparation of PLL electrode, 100% Triton is used.

About the protective layer, PLL is resolved in PBS to make 1mg/ml, 5mg/ml, 10mg/ml solution, and then get mixed with equal-volume 0.1% GA, incubate for 1min.

The enzyme solution was added in three portions, with 1 ul added each time. The protective layer solution was added in two portions, with 1 ul added each time. After the previous drop of solution has completely dried, add the next drop of solution.

## 2) Test of long-term preservation

Immerse the electrode in the PBS solution and measure the electrochemical signal after a few days.

## 3) Test of optimization with Neutralization

To ensure a sufficient cross-linking reaction, an excessive amount of GA was used. Therefore, even after the electrodes are prepared, there will still be a significant amount of aldehyde groups remaining on them. GA will spontaneously decompose under light conditions. However, when one aldehyde group has already reacted while the other has not, the aldehyde group will undergo an oxidation reaction alone and generate free radicals when exposed to air, which may be another reason for the degradation of the electrodes after long-term storage.

When immersed into solution, aldehyde tends to make crosslink reaction with amino group. While exposed in air, aldehyde tends to make oxidation reaction with oxygen, generating free radical, which may make damage to the enzyme layer and protective layer.

Glycine is the simplest amino acid, containing an amino acid, can serve as an object for participating in reactions involving aldehyde groups. So a glycine solution (0.4g/ml) is prepared, and several Neutralization schemes have been proposed:

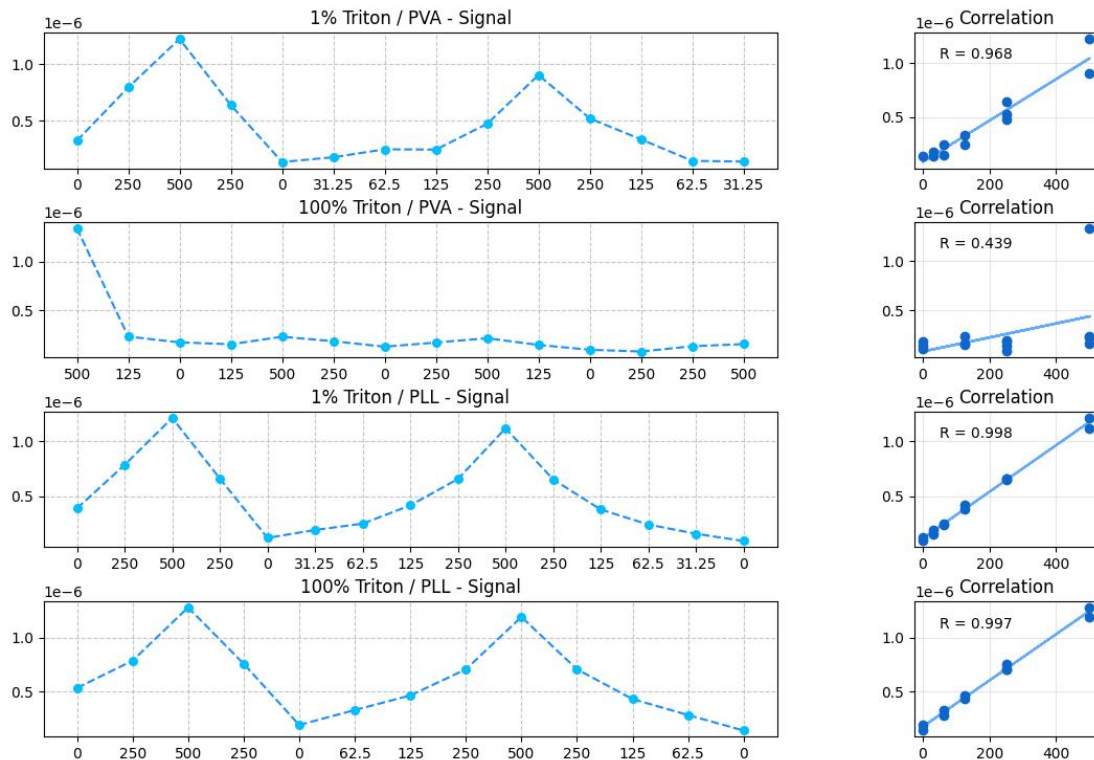
1. Prepare the electrode under room temperature
2. Neutralize the aldehyde after each layer's preparation, dropping 2ul glycine solution
3. Immerse the electrode into glycine solution immediately after the preparation of electrode
4. Leave the electrode in air after preparation for 30 mins, then, immerse the electrode into glycine solution immediately after the preparation of electrode

## Result

### PLL as protective layer can bear usage of higher concentration of Triton

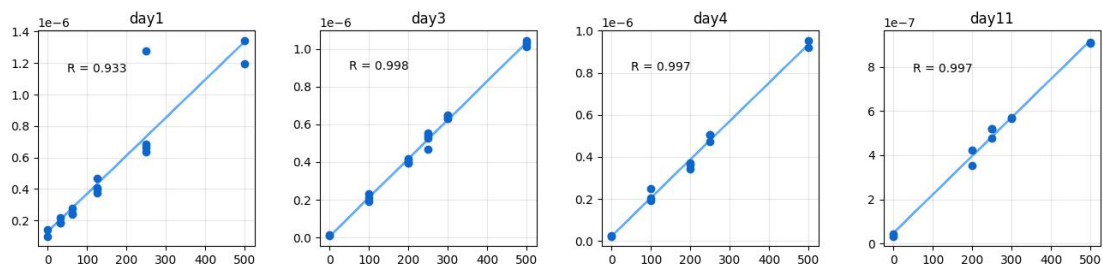
When mix the enzyme preparation protocol of PVA layer and PLL layer, results show that:

1. PVA layer can not hold the enzyme layer containing 100%Triton, while PLL layer has a good tolerance.
2. PLL protective layer has a better anti-degeneration ability than PVA, at least after the first round of testing



### PLL protective layer can provide long-term stability

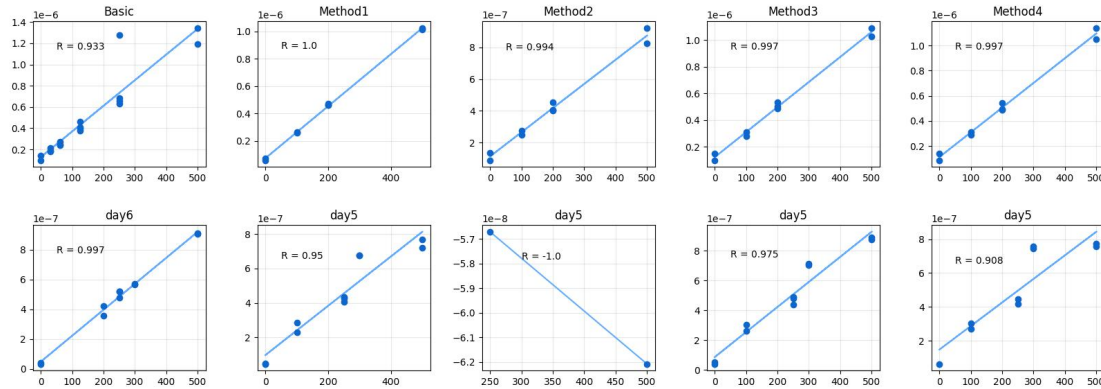
After long-term preservation in PBS, PLL electrode can maintain its stability and sensitivity. The highest signal appears at the first day, as a 1.4e-6 I current when testing 500mM creatinine. The signal of day3 and day4 are both 1e-6 I when testing 500mM creatinine. When it comes to day11, the signal decreases to 9e-7 I, indicating PLL protective layer holds a long-term preservation ability, and also, high ability.



### Closure of aldehyde does not help sensitivity



At first day, all electrodes show nearly the same sensitivity for creatinine. But after several days, the basic electrode without any neutralization of aldehyde takes the best performance in the correlation curve. All electrode except Method2, show a good current response.



## 8.3. Technical Details of the Electrochemical Sensing Platform

### 1. System Architecture

#### 1.1 Hardware Block Diagram

The system's architecture is modular, comprising two distinct parts: a single-use, disposable sensor strip and a durable, reusable electronic base. This design optimizes for both performance and long-term cost-effectiveness.

- Disposable Sensor Strip: This component consists solely of the three-electrode biosensor, which is replaced by the user for each new measurement session or after its operational lifetime.
- Reusable Electronic Base: This core unit houses all the electronics and is not disposable. It contains:
  1. Sensing Front-End (AFE): The TI LMP91000, which interfaces directly with the disposable sensor.
  2. Processing & Control Unit: An ultra-low-power MCU (e.g., STM32G4 series) that manages system operations.
  3. Wireless Communication Unit: The DX-BT24-T Bluetooth module for data transmission.
  4. Power Management Unit (PMU): An LDO and battery circuit that provides a stable 3.3V supply to the AFE, MCU, and Bluetooth module.

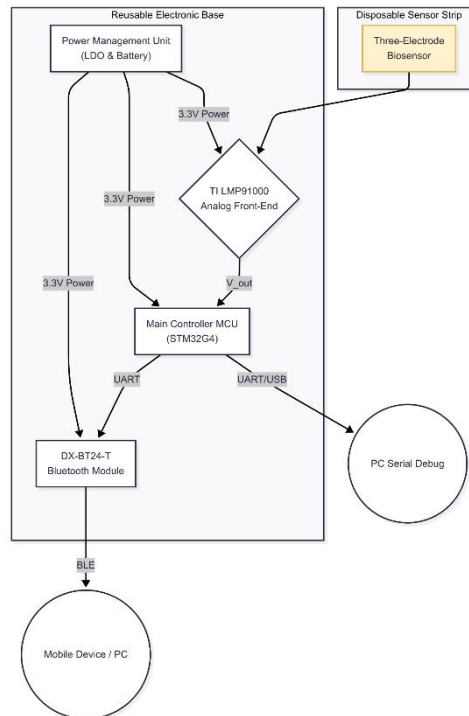


**Figure 1.** System Hardware Architecture.

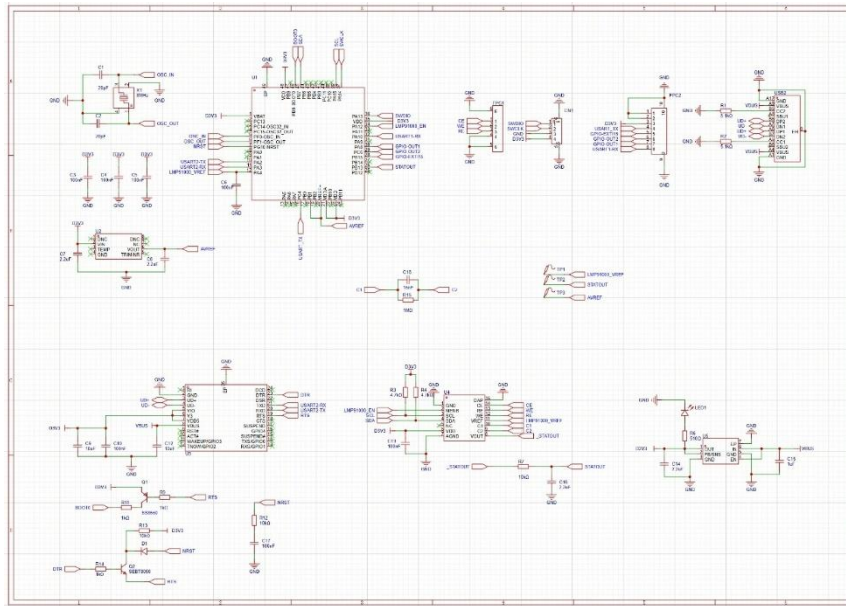


*Figure 2. System Schematic.*

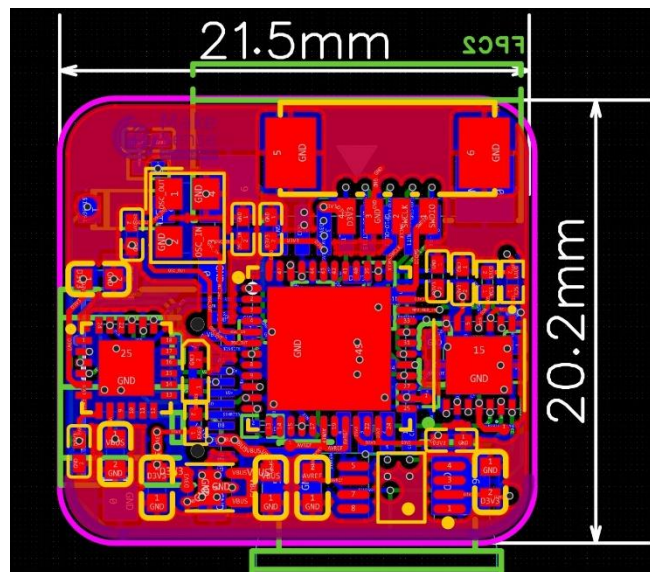


*Figure 3. PCB Layout.*

## 1.2 Firmware Architecture

The firmware is designed using a modular, layered architecture to enhance maintainability and portability. The firmware stack consists of three main layers:

1. **Hardware Abstraction Layer (HAL):** Encapsulates direct interactions with MCU peripherals (e.g., ADC, UART, I2C, Timers, GPIOs), providing standardized APIs to the upper layers.
2. **Drivers & Services Layer:**
  - **LMP91000 Driver:** Implements I2C-based read/write functions for all LMP91000 registers, providing APIs to configure bias voltage, transimpedance gain, etc.
  - **Data Processing Service:** Contains implementations of the ADC oversampling, Exponential Moving Average (EMA) filtering, and concentration conversion algorithms.
  - **Communication Protocol Service:** Manages the serialization and deserialization of data packets exchanged with the host application, based on a defined frame format.
  - **Power Management Service:** Implements the logic for entering deep sleep modes and waking up via a real-time clock (RTC) alarm for periodic measurements.
3. **Application Layer:** Orchestrates the top-level business logic using a **Finite State Machine (FSM)**. The FSM manages the device's primary states, including IDLE, SAMPLING, PROCESSING, TRANSMITTING, and SLEEP.

## 2 Detailed Hardware Implementation

### 2.1 Component Selection Rationale

- **Main Controller (MCU):** The STM32G473KBU6 was selected for its ultra-low-power performance, including multiple sleep modes with current consumption in the microampere range, which is critical for extending battery life. Its integrated 12-bit ADC and rich peripheral set meet all system requirements.
- **Analog Front-End (AFE):** The LMP91000 is a highly integrated potentiostat that significantly simplifies the analog circuit design. Its software-programmable bias and TIA gain allow for flexible adaptation to different sensor characteristics without hardware changes, reducing PCB footprint and complexity.
- **Bluetooth Module:** The DX-BT24-T module from DX-SMART TECHNOLOGY was selected for its pre-certified status, small form factor, and transparent serial

port profile (SPP), which simplifies firmware development by allowing the MCU to treat the wireless link as a simple UART connection.

- **Precision Voltage Reference:** A voltage reference IC (Texas Instruments REF5025) with a low temperature drift coefficient ( $< 10 \text{ ppm}/^{\circ}\text{C}$  (Instruments, 2023) ) and excellent long-term stability is used. It provides a constant, reliable reference for the ADC, fundamentally ensuring the accuracy and repeatability of measurements across varying environmental conditions.

### 3 Software Implementation Details

#### 3.1 Data Acquisition and Filtering Algorithm

- **ADC Oversampling:** To increase the effective number of bits (ENOB) of the measurement, the ADC is configured to acquire 256 consecutive samples for each data point. These samples are accumulated, and the result is right-shifted by 4 bits (an efficient division by 16). This process increases the effective resolution by 2 bits (from 12 to 14) and averages out high-frequency Gaussian noise.
- **Exponential Moving Average (EMA):** The oversampled data points are further smoothed using an EMA filter to suppress random noise and signal glitches. The filter is implemented with the recursive formula:  $Y[t] = \alpha \times X[t] + (1 - \alpha) \times Y[t - 1]$  Where  $Y[t]$  is the current filtered output,  $X[t]$  is the current input, and  $\alpha$  is the smoothing factor. A value of  $\alpha = 0.1$  is used, providing a robust balance between noise reduction and signal responsiveness.

## 8.4. Supplementary Data on an Alternative QCM Detection System Architecture

### Motivation

While the team initially explored and ultimately selected a three-enzyme electrochemical method, a comprehensive evaluation of alternative sensing platforms was conducted. One such platform was the Quartz Crystal Microbalance (QCM). Traditional QCM systems rely on designing and debugging a self-oscillating circuit that incorporates the QCM sensor itself. This approach presents several challenges:

1. **Complexity:** Oscillator circuits (e.g., Pierce, Colpitts) are sensitive to component variations and parasitic parameters, making them difficult to stabilize.
2. **Phase Noise:** The system's accuracy is often limited by phase noise, and precise phase measurement requires complex components like phase-locked loops (PLLs) or I/Q demodulators.
3. **Cost and Size:** The need for additional analog components for oscillation and phase detection increases the PCB footprint, component count, and overall system cost, hindering miniaturization for wearable applications.

To address these limitations, we analyzed an alternative architecture based on an open-loop frequency sweep and amplitude-only detection. This approach radically simplifies the hardware and software design.

### System Architecture and Principle of Operation

The proposed system eschews the self-oscillating paradigm in favor of a digitally controlled, open-loop measurement methodology. The architecture consists of four primary functional units, as illustrated in the conceptual block diagram (Figure 1).

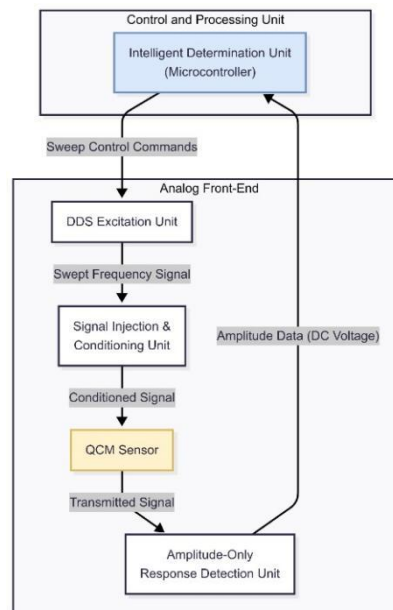


**Figure 1.** Conceptual block diagram of the open-loop QCM detection system based on frequency sweep and amplitude detection

1. **Direct Digital Synthesis (DDS) Excitation Unit:** This unit, controlled by a microcontroller (MCU), generates a high-resolution, swept-frequency sinusoidal signal. The MCU defines a precise frequency range (e.g., 9.9 MHz to 10.1 MHz) and step size (e.g., 10 Hz). This digitally synthesized signal replaces the analog oscillator, providing superior stability and control.
2. **Signal Injection & Conditioning Unit:** The output from the DDS is passed through a conditioning circuit, typically an LC filter network. This serves a dual purpose: it filters out high-frequency harmonics and DAC imaging artifacts from the DDS output, and it provides impedance matching to the QCM sensor, ensuring maximum and efficient power transfer.
3. **Amplitude-Only Response Detection Unit:** This is the core innovation of the system. Instead of measuring phase, it exclusively measures the amplitude of the signal transmitted through the QCM sensor. This is accomplished using a logarithmic amplifier/detector. As the excitation frequency is swept across the QCM's resonant point, the sensor's impedance changes dramatically, causing a distinct peak (or dip) in the transmitted signal's amplitude. The logarithmic detector converts this RF amplitude into a simple DC voltage, which can be easily measured by the MCU's Analog-to-Digital Converter (ADC).
4. **Intelligent Resonance Frequency Determination Unit:** The MCU orchestrates the entire process. It commands the DDS to step through each frequency, waits for the signal to settle, and then reads the corresponding DC voltage from the amplitude detector via its ADC. By associating each frequency step with its measured amplitude response, the MCU constructs a digital representation of the QCM's amplitude-frequency characteristic curve. Finally, a simple peak-finding algorithm is executed on this data array to pinpoint the exact frequency at which the maximum amplitude occurred. This frequency is identified as the QCM's resonant frequency.

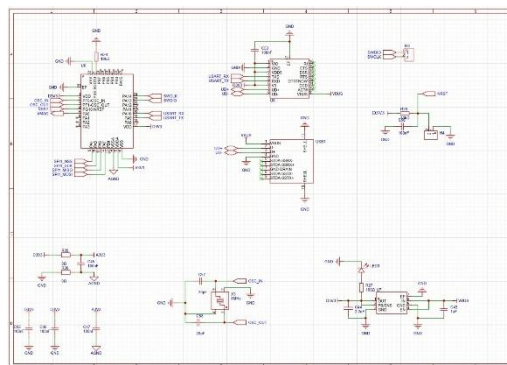
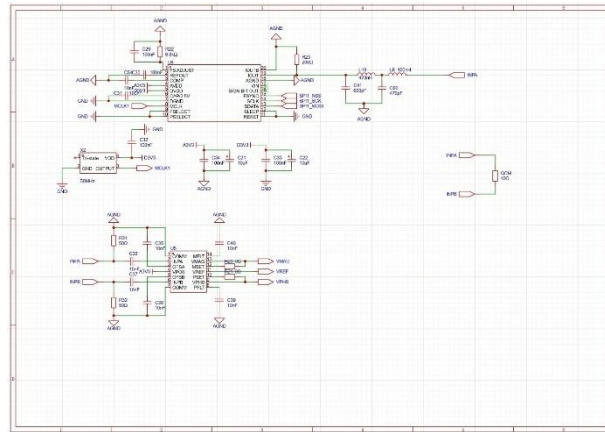


*Figure 2. System Schematic(Control & Processing Unit).*



## Key Advantages and Feasibility

This architecture offers significant advantages over traditional designs:

- **Hardware Simplification:** Eliminates the need for sensitive analog oscillator circuits, PLLs, and phase detectors, drastically reducing component count, PCB complexity, and potential points of failure.
- **Reduced Cost and Power:** Fewer active components and a simpler design lead to lower bill-of-materials (BOM) cost and reduced overall power consumption, making it ideal for portable and battery-powered devices.
- **Algorithmic Simplicity:** Determining the resonance frequency is reduced to a straightforward peak-finding search on an array of amplitude values, avoiding computationally expensive algorithms like phase unwrapping or complex curve fitting.
- **Enhanced Robustness:** The system is inherently less susceptible to environmental factors like temperature drift that can significantly impact the phase of a signal but have a less pronounced effect on amplitude peaks.



## 8.5. Creatinine — A Three-Compartment Blood – Sweat Convection-Diffusion Kinetic Model

### **Literature Review and Theoretical Basis**

In recent years, extensive theoretical and experimental research has been conducted, on the trans-compartment kinetics of small molecule biomarkers (such as glucose and urea) between blood plasma, interstitial fluid (ISF), and sweat (Yin, Adelaars, et al., 2025; Yin et al., 2023) . Classical multi-compartment pharmacokinetic models have been widely used to describe the diffusion, convection, and transport of molecules in different physiological compartments. For example, Yin's team and others have systematically proposed and improved a blood capillary-ISF-sweat gland (three-compartment) convection-diffusion kinetic model (Yin et al., 2023) . Combined with individualized parameter optimization and a double-loop inverse optimization strategy, they have successfully achieved highly accurate, noninvasive prediction of blood glucose and urea concentrations from sweat measurements. The model not only reproduces experimental measurements, but also achieves correlation coefficients (e.g., Spearman coefficient) above 0.98. This team has also developed optimization algorithms such as LDRW, which improve modeling efficiency and simplify the parameter system (Yin, Peri, Pelssers, Toonder, & Mischi, 2025) . It is worth noting that, although creatinine as a metabolic waste is not actively absorbed by cells in the interstitial fluid, its trans-compartmental kinetics are still highly consistent with the aforementioned small molecules in terms of passive diffusion, convection, and dilution mechanisms. In addition, recent work by Sophie Adelaars et al. has attempted to establish a multivariable regression model relating sweat creatinine concentrations & volume and plasma creatinine concentrations, with results demonstrating a certain degree of correlation between them (Yin, Adelaars, et al., 2025; Yin et al., 2023) . Together, these studies provide a theoretical and feasibility basis for creatinine trans-compartment kinetics modeling and noninvasive inference.

### **Model Structure and System of Governing Equations**

Based on the above theoretical foundation and literature support, we can employ a similar convection-diffusion three-compartment kinetic model (blood capillary-ISF-sweat gland) to quantitatively describe the transport, dilution, and kinetic processes of creatinine from the blood capillary through the ISF to the sweat gland duct. The model may mainly include the following governing equations:

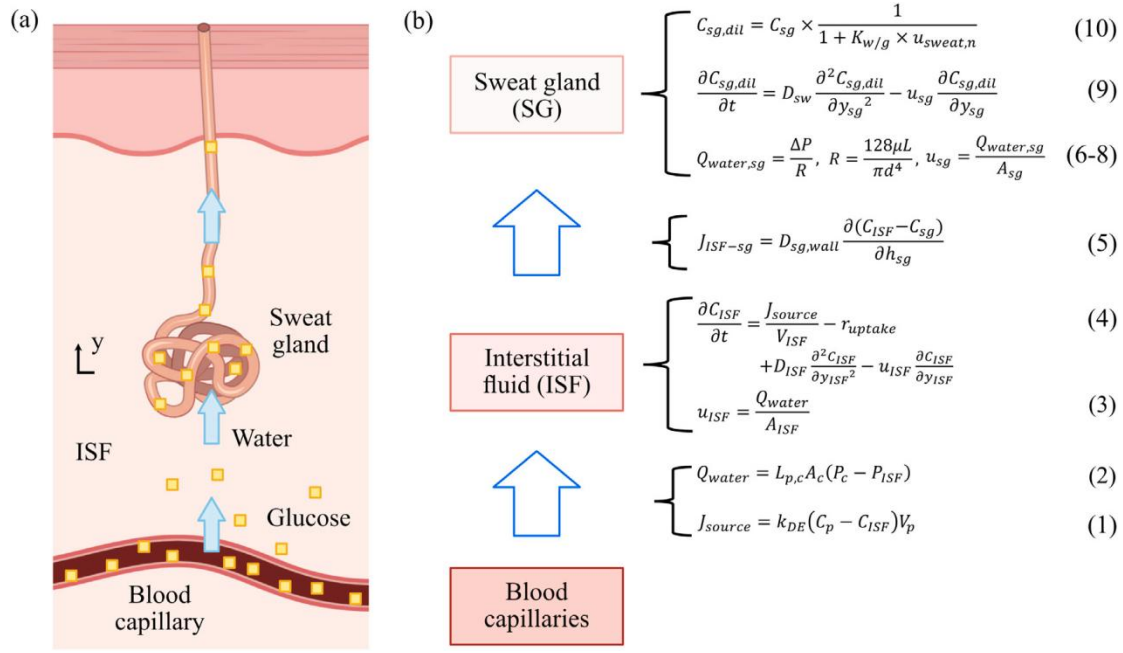


**Figure 1.** (a) Schematic of the glucose transport process from blood to sweat along a single sweat gland. (b) Compartment model and corresponding formulas.

- (1) Blood capillary–ISF transport:

$$J_{source} = k_{DE} (C_p - C_{ISF}) V_p$$

- (2) ISF Water Flux

$$Q_{water} = L_{pc} \cdot A_c \cdot (P_c - P_{isf})$$

- (3) ISF Convective Velocity

$$u_{ISF} = \frac{Q_{water}}{A_{isf}}$$

- (4) ISF convection-diffusion kinetics:

$$\frac{\partial C_{ISF}}{\partial t} = \frac{J_{source}}{V_{ISF}} + D_{ISF} \frac{\partial^2 C_{ISF}}{\partial y^2} - u_{ISF} \frac{\partial C_{ISF}}{\partial y}$$

- (5) ISF–sweat gland wall diffusion (Fick's first law):

$$J_{ISF-sg} = D_{sg,wall} \frac{C_{ISF} - C_{sg}}{h_{sg}}$$

- (6) Sweat Gland Hydraulic Resistance (Darcy's law)

$$R_{sg} = \frac{128\mu L_{sg}}{\pi d^4}$$

- (7) Sweat Gland Water Flux

$$Q_{sg} = \frac{\Delta P}{R_{sg}}$$

(8) Sweat Gland Convective Velocity

$$u_{sg} = \frac{Q_{sg}}{\pi(d/2)^2}$$

(9) Sweat gland duct convection-diffusion kinetics:

$$\frac{\partial C_{sg}}{\partial t} = D_{sw} \frac{\partial^2 C_{sg}}{\partial y^2} - u_{sg} \frac{\partial C_{sg}}{\partial y}$$

(10) Dilution correction at sweat gland outlet:

$$C_{sg,dil} = \frac{C_{sg}}{1 + K_{w/g} \cdot u_{sweat,n}}$$

### Individualized Inverse Problem Optimization Strategy

To achieve noninvasive inference of blood creatinine concentration from sweat measurements, inspired by the work of Yin et al. in the field of glucose modeling and inverse optimization, we can employ an “individualized parameter – input double-loop optimization” strategy, as follows:

Loop 1 (input inner loop): Optimization of the input blood creatinine time series, minimizing the error between the model-predicted and experimentally measured sweat creatinine concentrations, to yield the optimal blood creatinine input sequence.

Loop 2 (parameter outer loop): Based on the optimized input from Loop 1, person-specific calibration of key model parameters (such as diffusion coefficients, dilution coefficients, sweat flow rate parameters, etc.), further improving the model fit to each individual’s physiological characteristics.

Objective function: The overall optimization goal is to minimize the mean squared error (MSE) between the model output and the measured sweat creatinine concentration.

### Sweat Flow Rate Parameter

Sweat flow rate, as a key parameter affecting the dilution and dynamic changes of small molecule concentration in the sweat gland, is explicitly incorporated into the model. In recent years, the rapid development of microfluidic sweat collection and sensing technology has provided us with feasible methods for in situ, real-time measurement of sweat flow rate. By integrating electrode impedance, electrochemical, or optical sensors in microfluidic channels, it is possible to accurately monitor the volume of sweat per unit time, realize dynamic tracking of sweat rate, and input it into the model for individualized parameter calibration and dynamic modeling. This lays a theoretical and technical

foundation for subsequent joint modeling of sweat flow rate and creatinine (and other biomarkers), as well as high temporal – spatial resolution sweat kinetics analysis.

### **Method Outlook and Explanation**

It should be pointed out that the schemes and methods described in this appendix are still at the stage of feasibility demonstration. Some steps have not yet been fully implemented in this project, but they provide a complete theoretical foundation and feasibility reference for future work on high-precision sweat kinetics modeling, real-time sweat flow collection, and individualized health monitoring.

## 8.6. Microfluidic Design

### Sample Injection System

The microfluidic sample injection system, as illustrated in Fig. a, consists of a sample reservoir, connecting tubing, and a polydimethylsiloxane (PDMS) reaction chamber with a volume of approximately 40  $\mu\text{L}$ . On the injection side, an upper-wide and lower-narrow sample reservoir (capacity: 150  $\mu\text{L}$ ) was employed to minimize the contact area between successive samples. This configuration allowed the introduction of the next sample just before the previous one was depleted, thereby reducing inter-sample mixing. On the outlet side, a microinjection pump was used to draw liquid from the chamber at a rate of 100  $\mu\text{L}/\text{min}$ , replacing it with the next sample. The PDMS layer was designed to be as thin as possible so that under negative pressure the effective chamber volume was minimized, further improving replacement efficiency. The first extraction was used for rinsing, continuously withdrawing 40  $\mu\text{L}$  (Fig. a), followed by a second extraction for testing, withdrawing 40  $\mu\text{L}$  (Fig. a). Additional measures, such as continuously withdrawing at 300  $\mu\text{L}/\text{min}$  for 5 s, could be implemented to completely remove residual liquid from the channel. At this point, approximately 20  $\mu\text{L}$  remained in the sample reservoir; considering the diffusion-induced contamination of this residual liquid, from the second extraction onward, each cycle withdraws 40 + 20  $\mu\text{L}$  to account for the portion of liquid in the sample reservoir affected by diffusion.

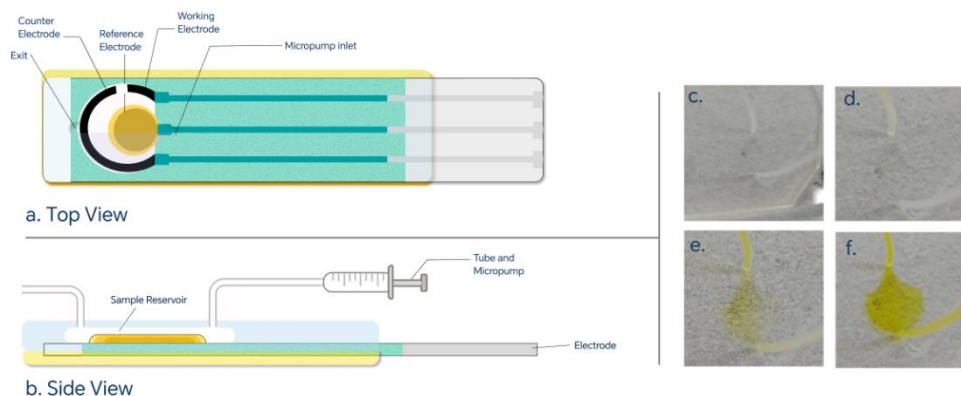


**Figure a.** Primary Sample Injection System.

This design minimizes sample mixing not only through operational optimization but also through chip geometry refinement. While maintaining a small chamber volume, large-radius curves were extensively adopted to reduce hydrodynamic resistance, the transition channel lengths were shortened, and all corners were chamfered to avoid boundary layer separation and backflow that could compromise flow stability and controllability. The validity of these design strategies was experimentally verified using two differently colored liquids (Yellow and Colorless, Fig. a), demonstrating minimal mixing after sample replacement.

### Improved Sample Injection System

When using standard commercial electrodes, the surface processing may not ensure reliable bonding with PDMS. For more widely used standardized electrodes, we developed a revised design tailored to the electrode–fluid interface. In this configuration, most microfluidic channels maintain a uniform width to suppress boundary layer separation and turbulence. The reaction chamber volume was further reduced, enabling higher-frequency detection in real-world applications. The implementation involved three representative steps: (1) injection (with injection volumes indicated in Fig. b ) ; (2) replacement in progress; and (3) complete replacement. As shown in Fig. b, similar replacement efficiency was achieved with less liquid volume, demonstrating the potential of this approach for low-volume, high-frequency sensing.

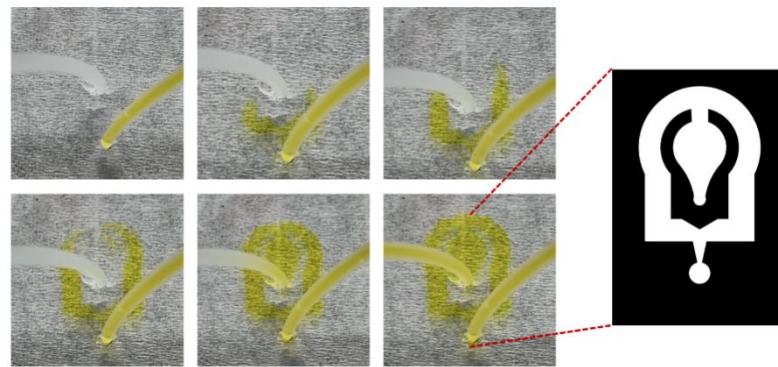


*Figure b. Improved Sample Injection System.*

### Single–Channel Sweat Microfluidic System

The single-channel sweat collection system combines natural sweat gland pressure with optimized capillary forces and an evaporation pump to ensure high temporal resolution and accuracy, in which, besides using the sweat gland itself as the pressure source, the optimized capillary action and evaporation pump are simultaneously introduced to activate sweat flow. At the inlet, a multi-pillar structure serves as the sweat entry point, preventing deformation-induced flow instability and filtering out particulates to avoid clogging the capillary network. Downstream, the capillary channel provides an additional driving force and ensures unidirectional flow. Chamfered capillaries help maintain uniform velocity and enhance throughput, consistent with literature reports. The rear circular chamber (diameter: 10 mm) is designed to accommodate the sensing electrodes, followed by a waste outlet zone containing hydrophilic porous material to accelerate liquid removal via evaporation.

After passing through the detection zone, creatinine in the sweat diffuses to the sensing electrodes, triggering a three-enzyme cascade reaction. The entire sweat sensor was fabricated on a glass substrate, with PDMS used for its excellent biocompatibility, enabling direct application to skin surfaces. In operation, a microinjection pump delivered the test fluid into the chamber at 100  $\mu\text{L}/\text{min}$ . When 70  $\mu\text{L}$  was injected, the electrodes were fully wetted, and excess liquid flowed into the outlet without retention or overflow (Fig. c), ensuring real-time monitoring of fresh sweat that reflects the true physiological state. A complete sweat sensing system was then constructed, which could be preloaded with simulated sweat samples for validation, allowing accurate monitoring of biomarker concentrations in agreement with reference methods.

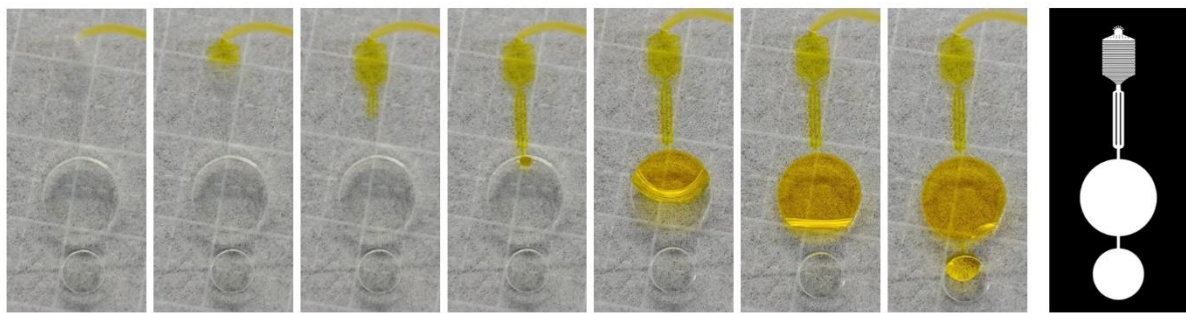


*Figure c. Single-Channel Sweat Microfluidic System.*

### **Multi-Channel Sweat Microfluidic System**

The multi-channel sweat microfluidic system integrates three single-channel units in parallel, with reduced electrode surface areas (5 mm diameter) for enhanced portability. The parallel configuration ensures similar spatial orientation of all sensors under real-world conditions, minimizing gravity-induced bias in measurements. Each channel is paired with detection electrodes targeting different biomarkers, and the post-reaction fluids are directed into a common waste outlet zone. A check capillary bursting valve is positioned upstream of the outlet zone to prevent cross-contamination between chambers. This system, also fabricated on a glass substrate with PDMS-based microchannels, was validated using preloaded simulated sweat samples, demonstrating accurate multi-analyte detection under controlled conditions (Fig. d). we also constructed the same skin-conformable flexible microfluidic sweat sensor model as described above.

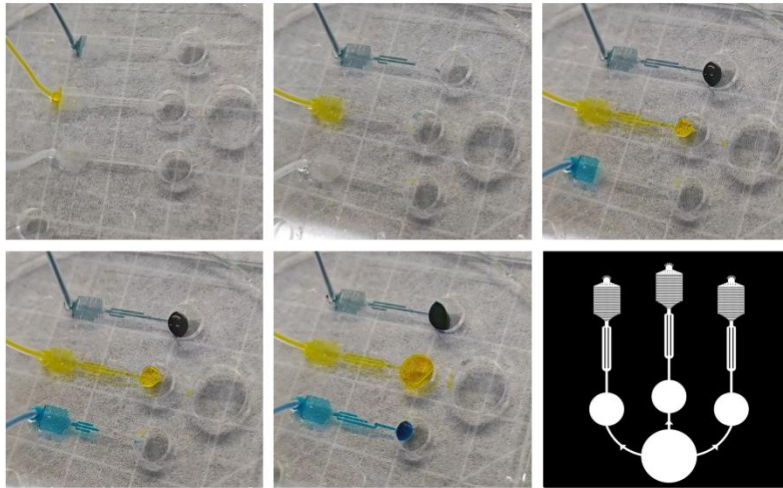


*Figure d. Multi-Channel Sweat Microfluidic System.*



## 8.7. Software Design

While the MakeSense hardware addresses the pain points of traditional detection methods, such as invasiveness and latency, *Creasense*, an intelligent monitoring application, solves software challenges: eliminating dependency on chemical workstations, enabling direct device connection, and providing real-time data visualization. Core innovations include a dynamic protocol engine that supports zero-release hardware or software upgrades, a BLE state machine ensuring connection stability, and local privacy protection compliant with medical and commercial regulations. The current implementation includes cross-platform architecture, internationalization for 5 languages and easy-nd interfaces, and developer tools. The source code and technical documentation to-*exte* are open-sourced on GitHub ([CNDYI390/Creasense: Sense Your Creatinine - Advanced cross-platform creatinine monitoring application](https://github.com/CNDYI390/Creasense: Sense Your Creatinine - Advanced cross-platform creatinine monitoring application)).

### 8.7.1 Basic Info

Our software is named *Creasense*, a name that embodies a profound medical technology philosophy. "Crea" is a prefix for Creatinine, and "Sense" signifies perception/monitoring. Together, it means "Sense Your Creatinine". Our goal is not just to create a demo, but to develop a fully functional and polished product, ultimately for release on the App Store. The software utilizes a modern architecture and design to ensure it is efficient, lightweight, smooth, user-friendly, and extensible.

1. Mission: To advance user experience with modern technology.
2. Vision: To bring kidney function monitoring from hospitals to daily life, safeguarding your health through non-invasive and minimally invasive intelligent detection, becoming a globally leading portable biomarker monitoring platform, and promoting the popularization of precision medicine.
3. Values: Privacy First (local processing), Openness and Transparency (open-source verification), Continuous Innovation (dynamic protocol), User-Friendliness (accessible design).

### Visual Presentation



Creasense Icon Default



Creasense Icon Dark



Creasense Icon on iOS 26

*Figure 1 .Icons of Creasense.*

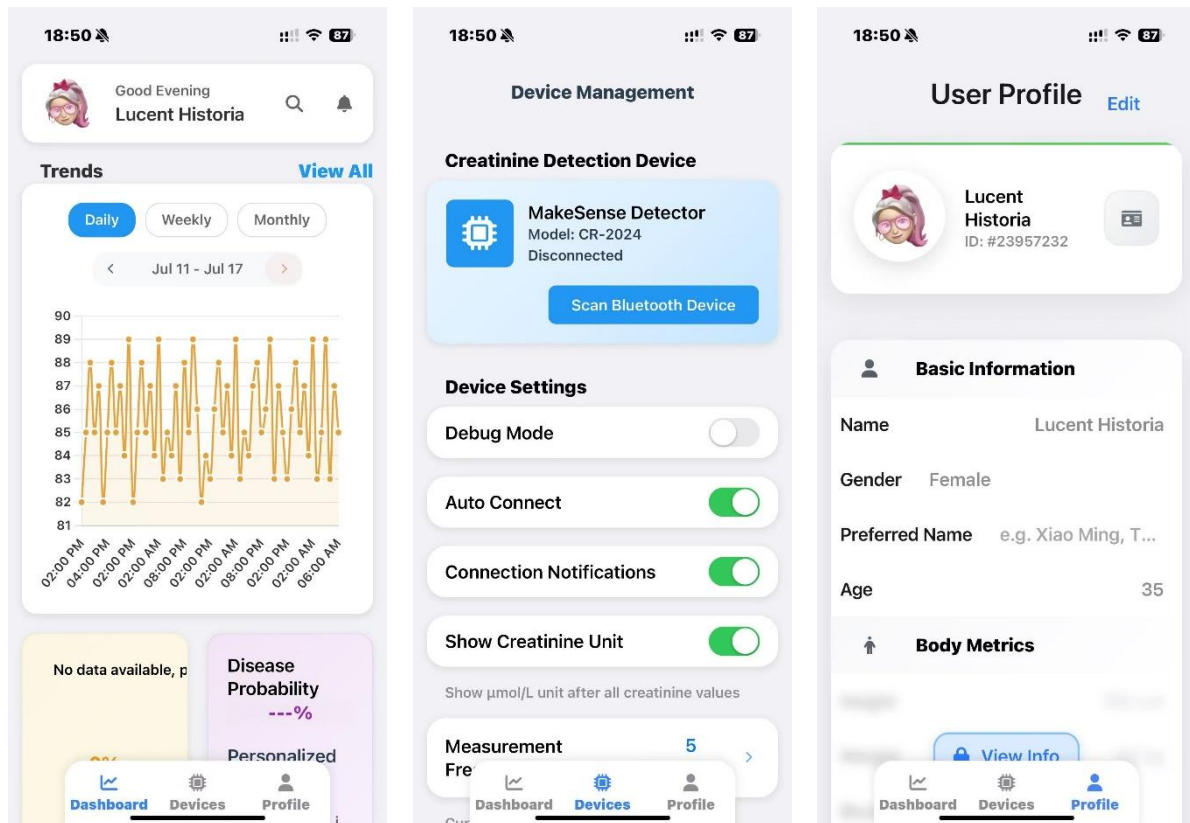


*Figure 2. Screenshots of Creasense (on iPhone 15 Pro).*

## Highlights & Features

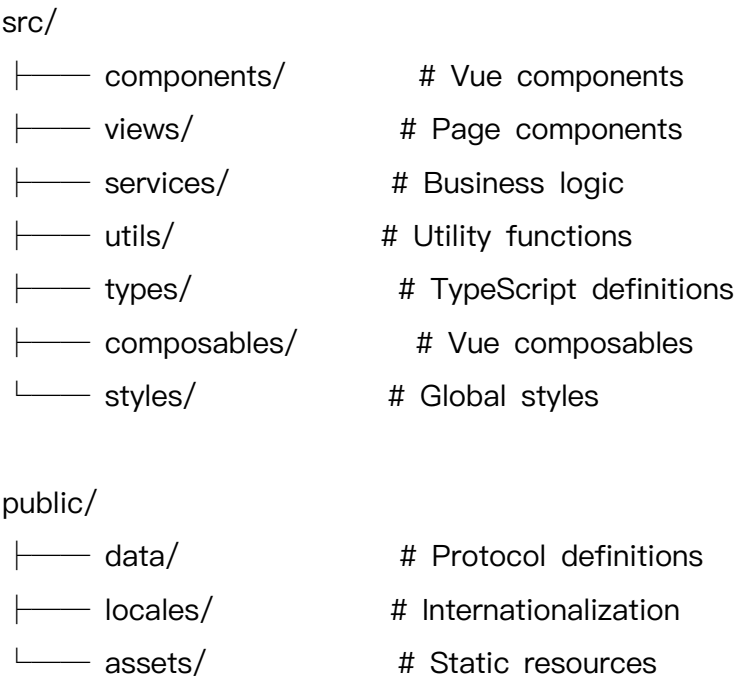
1. **For Daily Use:** Direct wearable-to-app communication, eliminating the need for a chemical workstation.
2. **Commercial Ready:** Adheres to Apple HIG and is App Store compliant. Open-source for transparency, with Face ID for data protection.
3. **Globalization Ready:** Native multilingual support with resource-based files for easy expansion. English, Dutch, and more are already supported.
4. **Efficient Protocol:** Employs bitwise flags for dynamic field recognition and hot-reloading to ensure forward/backward compatibility.

- 5. **Native Cross-Platform:** Built on Vue3 + Capacitor for a single codebase that delivers a consistent experience across all platforms.
- 6. **Refined User Experience:** Thoughtful micro-interactions and optimizations for enhanced efficiency.

8.7.2 System Architecture Design

The system is based on a modular design philosophy, ensuring code maintainability and scalability.

System Layer Overview



Layer	Tech Stack	Responsibility
UI Layer	Vue3 + Ionic8	User interface, interaction logic
Business Layer	TypeScript Services	Device management, data processing
Data Layer	Local Storage + Pinia	State management, persistence
Platform Layer	Capacitor7	Native API bridging
Protocol Layer	Dynamic Protocol Engine	Packet parsing, compatibility

Main Module Responsibilities:

1. services/: Core business logic (BLE management, data storage, biometric authentication)
2. utils/: Utility functions (protocol parsing, chart data aggregation, platform adaptation)
3. views/: Page components (Dashboard, Devices, Developer, Profile)
4. composables/: Composables API (multilingual support, text selection, protocol configuration)

## **Software Technology Stack**

### **1. Frontend Framework Layer**

Utilizes web technology stack to achieve cross-platform capabilities. The first phase prioritizes development for the iOS platform, with subsequent rapid adaptation for Android and Web.

- Vue 3 Composition API
- TypeScript
- Ionic 8
- Vite 7

### **2. Mobile Packaging Layer**

Adopts the advanced packaging tool Capacitor 7 to ensure minimal package size, performance, startup speed, and user experience.

### **3. State Management and Routing**

- Pinia: The officially recommended state management solution for Vue 3, with a more concise API design.
- Vue Router 4: Supports history mode and scroll position preservation to enhance user experience.

## **Hardware–Software Integration Layer**

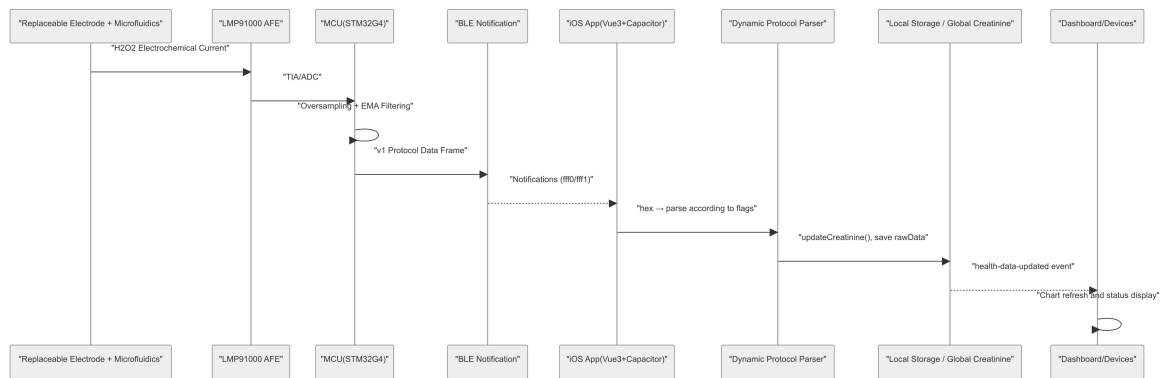


**Figure 3.** Data Pipeline.

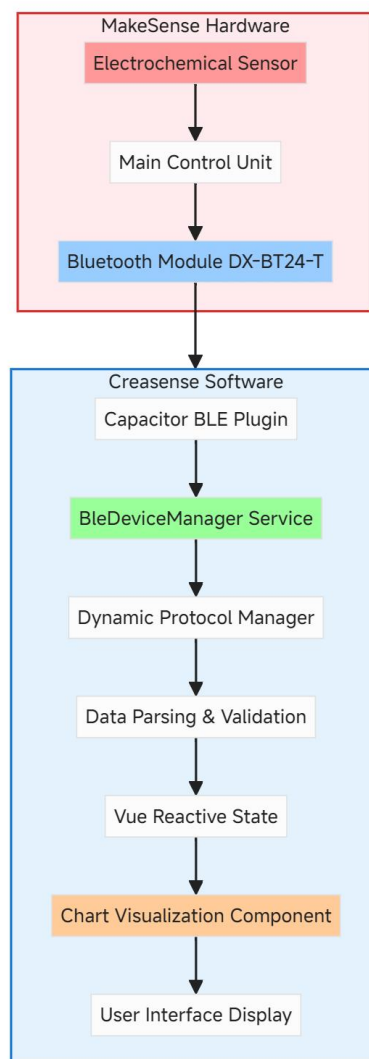


**Figure 4.** Data Flow.

1. Hardware: Sensor → AFE → MCU → Bluetooth Module
2. Communication: Bluetooth protocol → Capacitor plugin bridging
3. Application: TypeScript service → Reactive state management

4. Presentation: Vue component → Chart.js visualization

### Communication Protocol Stack

Our system implements a complete Bluetooth Low Energy (BLE) communication protocol stack, ensuring stable and reliable communication between the mobile application and the hardware device.

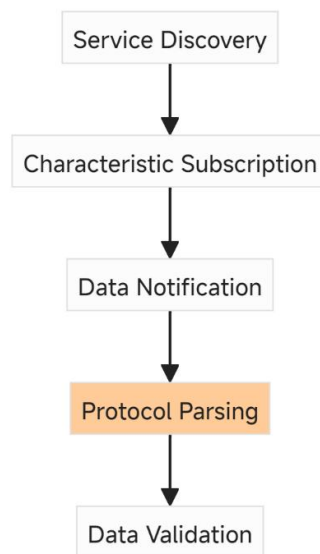


*Figure 5. Bluetooth Procedure.*

### 8.7.3 UI Layout and User Experience

#### App User Flow Chart

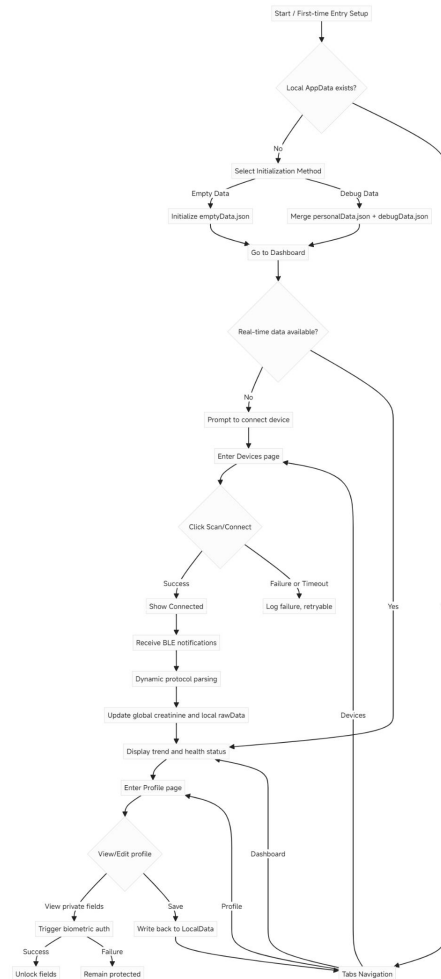


*Figure 6. App User Flow Chart*

## Page Design

### 1. Dashboard - Health Overview & Trends

#### • Real-time Health Overview

- A dynamic ring graph intuitively displays the current creatinine concentration, corresponding health level, and percentage.
- The system automatically calculates and provides a graded assessment based on the data (e.g., Normal, Mild, Moderate, Severe).
- Offers intelligent health status assessments and potential risk alerts.

#### • Multi-dimensional Trend Analysis

- Supports switching between daily, weekly, and monthly views, with custom date range navigation for analyzing data across different time spans.
- Charts can display detailed data points from the last 24 hours, average values and fluctuation ranges for the last 7 days, and long-term trends over 30 days.

#### • Intelligent Data Aggregation & Interaction

- Utilizes Chart.js to dynamically adapt the chart's y-axis and optimizes performance with a 5-minute caching mechanism.
- Allows users to tap on individual data points to view detailed information, such as measurement time and environmental parameters.

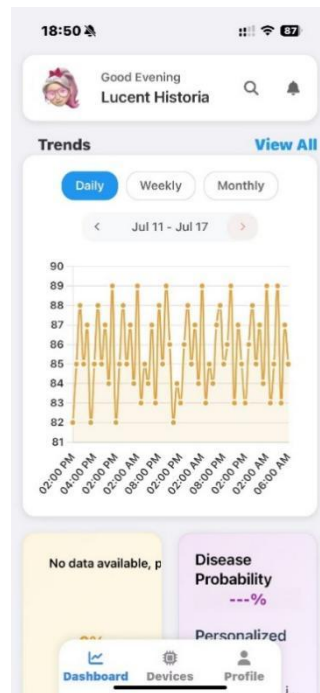


*Figure 7. Dashboard View*

## 2. **Device Management (Devices) - Connection & Configuration**

### • **Intelligent Connection Management**

- Employs a state-machine-driven process (IDLE → CONNECTING → CONNECTED) to ensure a stable and reliable connection workflow.
- Features a smart 15-second scan timeout and an automatic cleanup-and-reset (cleanupAndReset) strategy upon failure.

### • **Comprehensive Device Information & Logs**

- Records a timestamped, end-to-end connection log and provides statistics on connection successes and failures.

### • **Personalized Parameter Configuration**

- Allows users to customize settings such as auto-connect, measurement frequency, and creatinine unit display.
- Developer Mode can be accessed by tapping 5 consecutive times in the settings interface.



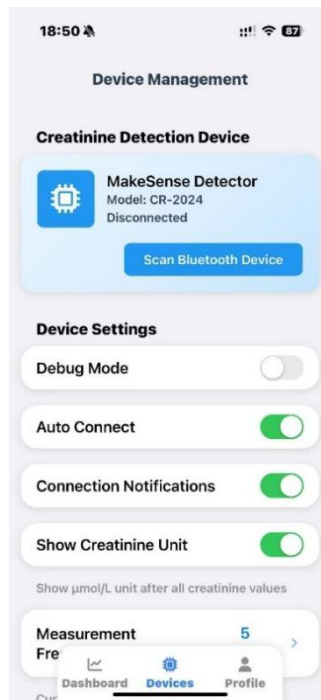


*Figure 8. Device View*

### 3. **Developer Tools (Developer) - Debugging & Testing**

- **Activation Method**

- This interface is hidden by default and can be accessed by tapping 5 consecutive times on the Device Management page.

- **Dynamic Protocol Management**

- Supports loading, validating, and switching between different communication protocol files at runtime.
- Allows developers to import custom protocols for testing purposes.

- **Communication & Parsing Debugging**

- Supports sending custom HEX or text data to test hardware responses.
- Monitors incoming data packets in real-time and presents parsing results in a categorized list (success/error).

- **Device Calibration & Diagnostics**

- Provides a tool interface for device calibration (e.g., metric calibration).
- Supports the management of device batch coefficients.

### 4. **Profile - Privacy & Management**

- **Personal Health Profile**

- Users can manage basic information (age, gender, height, weight) and medical history (past conditions, medication usage).

- Supports adding and managing emergency contact information.
- **Biometric & Privacy Protection**
  - Sensitive data, such as body metrics and medical information, is masked by default.
  - Viewing this data requires unlocking via Face ID or other biometric technologies, with a 30-second unlock validity period.
  - Adheres to the "minimal privacy principle," storing only necessary fields locally and providing a "Clear All Data" option.
  - Profile pictures are processed locally and are not uploaded to the cloud to protect user privacy.
- **Medical ID Card**
  - In an emergency, critical medical information (e.g., allergies, regular medications, contacts) can be quickly displayed. Accessing the card generates a view log.
- **Application Settings**
  - Provides a multi-language switching function.

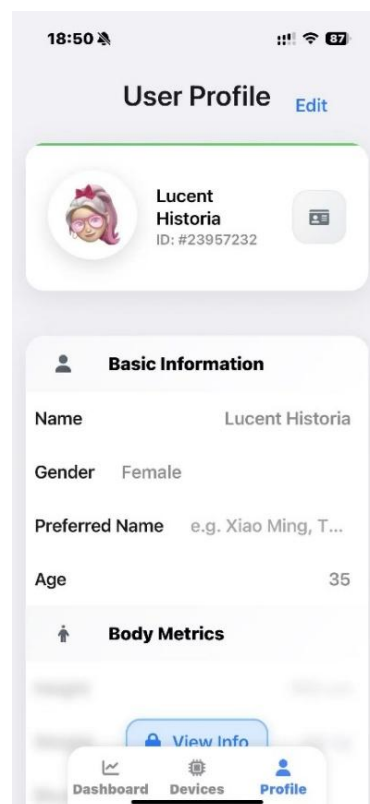


*Figure 9. Profile View*

## 5. Setup (Initialization)

- Purpose & Trigger
- Core Functions

#### 8.7.4 Core Function Implementation

##### Interface and Internationalization

Composition API, custom CSS, unified Apple font family; multi-language JSON resources loaded on demand (useI18n.ts).

##### Navigation and Experience

Tabs layout implements a single-page, single-route model, scroll position preservation (router/index.ts), connection history, and event-driven UI updates.

##### Communication Protocol Design

To support firmware upgrades and protocol changes for the hardware device, we designed a dynamic protocol management system to achieve software-hardware version compatibility.

##### V1 Protocol (12 bytes)

1. flag: 1 byte (8 bits) for protocol extension and cross-version identification.
2. sensorStatus: 1 byte to monitor sensor status.
3. batteryVoltage: 2 bytes to reflect battery level.
4. timestamp: 4 bytes for calculating latency and saving time-series data.
5. current: 4 bytes to measure current, reflecting creatinine concentration.

Field	Type	Range	Max Value	Max Value	Requirement
flag	uint8	[0]	0b11111111	—	Extension bits + sign bit
Sensor Status	uint8	[1]	255	—	/
Battery Voltage	uint16	[2~3]	65535	0-65.535 V	3.500V-3.800V
Unix Timestamp	uint32	[4~7]	4294967295	—	Little-endian, Jan 1, 1970 ~ 2106
Current	uint32	[8~11]	4294967295	0-429496.7295nA	100.0000nA-1000.0000nA

## Protocol File

```
{
  "protocolLength": 12,
  "comment": {},
  "flags": {
    "bit0": {
      "name": "sensorStatus",
      "type": "uint8"
    },
    "bit1": {
      "name": "batteryVoltage",
      "type": "uint16_le"
    },
    "bit2": {
      "name": "timestamp",
      "type": "uint32_le"
    },
    "bit3": {
      "name": "current",
      "type": "uint32_le"
    },
    "bit4": {},
    "bit5": {},
    "bit6": {},
    "bit7": {}
  }
}
```

## Protocol Parsing Algorithm

This algorithm is based on the **bitwise AND (&) operation**, using a flag byte for efficient, maintainable, and highly extensible code-level parsing.

Our protocol engine uses an 8-bit flags design, where each bit corresponds to the existence of a data field. Dynamic field recognition is achieved through the **bitwise AND (&) operation**:

```

for (let bit = 0; bit < 8; bit++) {
  const flagMask = 1 << bit;
  const isFlagSet = (flags & flagMask) !== 0;
  if (isFlagSet) {
    const bitKey = `bit${bit}`;
    const fieldDef = protocol.flags[bitKey];
    const value = this.readFieldValue(view, offset, fieldDef.type);
    parsedData[fieldDef.name] = value;
    offset += this.getFieldSize(fieldDef.type);
  }
}

```

If the app's parsing program were hardcoded to only recognize the V1 packet format, it would completely fail to understand V2 or V3 packets. It might even misread other data, such as "body surface temperature," as a "timestamp," causing the entire system to crash.

**Instead, we use a flag byte (8 flag bits)** for intelligent packet reading. When the app receives a packet, it first reads the flags and then "disassembles" the packet strictly according to the bitmap, achieving high extensibility and forward/backward compatibility.

## 8.7.5 Privacy, Security, and Development Compliance

### Data Privacy Protection System

We have built a comprehensive privacy protection system that strictly adheres to the "principle of minimum privacy" and international standards like GDPR:

1. Biometric Gate: Viewing/editing private fields requires Face ID; failure keeps them locked. Users are passively shown a prompt and can navigate to system settings to grant permission.
2. Minimal Necessary Storage: Only raw measurement values and basic user profile are stored locally; sensitive information is viewed only locally, masked by default, and requires authentication to view.
3. Logging Strategy: Only local debug logs; all errors are explicitly logged via `console.error`, not silently suppressed.
4. Revocability: Profile supports one-tap clearing of local data; Setup supports reset; navigation guards guide the user back to initialization if data is missing.

### Compliance and Platform Guidelines

## **Apple Ecosystem Compliance**

1. Human Interface Guidelines Adherence: Safe area adaptation, handling of special areas like the notch and Dynamic Island.
2. Dynamic Type Support: Adheres to iOS system font size settings for accessibility optimization.
3. App Store Review Requirements: Medical/Health category, content rating follows iOS 26 guidelines, comprehensive privacy policy.

## **Permission Requests and Usage Descriptions**

1. Bluetooth: Used only for communication with the wearable reader.
2. Face ID: Used only for unlocking local private fields.
3. Photo Library: Used only for changing the avatar, with no other access requirements.

## **Basic Strategy**

1. Default Lock: All private fields are locked by default.
2. Authentication Timeout: Biometric re-authentication is required after 30 seconds.
3. Edit Relock: All fields are forcibly relocked after an edit operation is completed.
4. Page Cleanup: All unlocked states are automatically cleared when the page is exited.

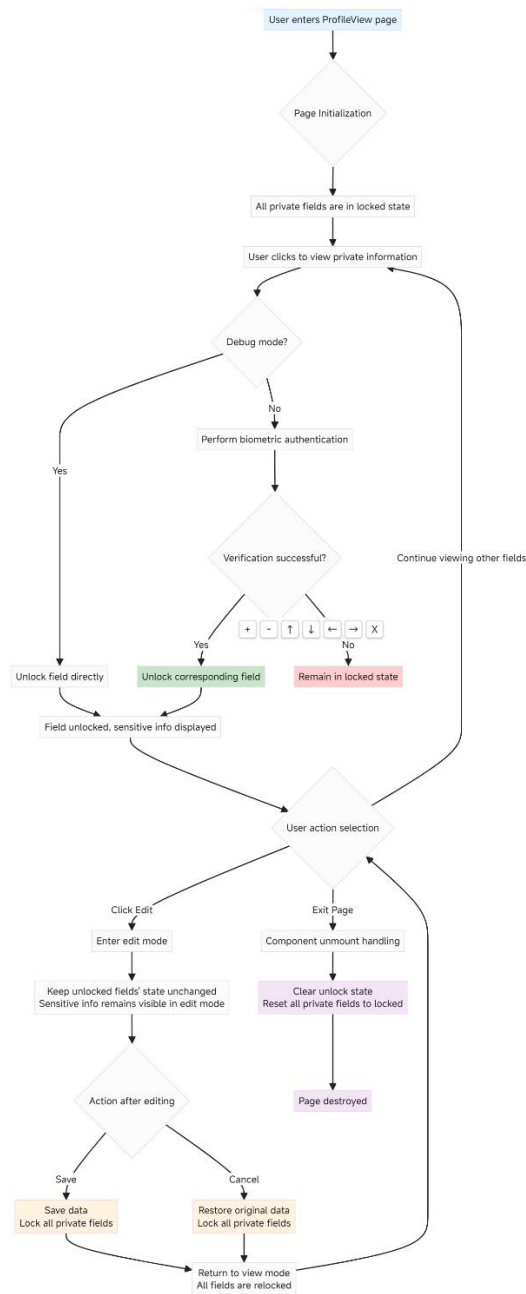


*Figure 10. User Operation Flow Chart*

## Apple Ecosystem Compliance Design

### 1. Human Interface Guidelines (HIG) Adherence

Safe area adaptation, adapting to iPhone notch, Dynamic Island, and other special areas.  
System font adaptation, adhering to iOS dynamic font size settings.

### 2. App Store Review Compliance

- Permissions and Usage Descriptions:
  - Bluetooth: Used only for communication with the wearable reader; purpose explained in system permission pop-ups and App Store description.

- Biometric: Used only for unlocking local private fields; provides a redirect to settings on failure.
- Photo Library: Used only for changing the avatar, processed locally and not transmitted.
- Font Unification and Typography: Globally uses the Apple font family (e.g., -apple-system family with headline/body/footnote hierarchy), font sizes and line heights follow human factors best practices.
- Safe Area and Responsiveness: Adheres to safe area layouts, keeping important interactions away from edges; adaptation for large-rounded-corner devices and notched devices is achieved through containers and padding.
- Logging Strategy: Only logs necessary information and errors; the competition version will not introduce external tracking or uploading.
- Content rating compliant with the latest iOS26 guidelines.

#### **8.7.6 Medical Compliance Disclaimer**

- Protocol Field Units and Scaling: battery Voltage (mV), current (0.0001 nA) , creatinine ( $\mu\text{mol/L}$ ).
- **Disclaimer: The data provided by this sensor and the suggestions provided by this App do not constitute a basis for clinical diagnosis.**

#### **8.7.8 Complete Code Structure**

For the complete code structure, please see the GitHub repository ([CNDY1390/Creasense](https://github.com/CNDY1390/Creasense)).



## 8.8. Translational Potential

### 8.8.1. Pre-interviews & desk research (themes and key insights)

We first conducted preliminary desk research and expert pre-interviews on creatinine-related kidney diseases to understand the clinical context, define key issues, and build the framework for formal interviews. At each pre-interview's conclusion, we outlined long-term project aims and invited suggestions from physicians and nurses. From two nephrologist and two nephrology nurse pre-interviews, key insights included: Acute kidney injury (AKI) is common in tertiary hospitals, with ICUs handling about 2–5 cases daily; acute and chronic kidney disease practitioners interact little. AKI arises mainly in ICUs, with sudden onset, unpredictable course, and rapid deterioration; CKD progresses slowly in nephrology wards. AKI patients often have weakened mental states during hospitalization; ICU physicians and nurses are essential sources for first-hand AKI observations.

### 8.8.2. Interview subjects & execution details

In the Chinese market context, interviewees spanned nephrologists in tertiary hospitals from various city tiers, experienced nephrology nurses, kidney-disease patients and families, and policy/regulatory authorities. Examples include a nephrologist with 20 years' experience and a veteran nurse for clinical perspectives, as well as early- to mid-stage CKD patients and families for lived-experience insights. Interviews were one-on-one, each ~30 minutes, with key points recorded upon participant consent. We maintained a smooth conversational flow and built rapport in the closing stage to foster trust. This approach yielded rich, authentic first-hand data, forming a solid basis for product design and market positioning.

### 8.8.3. Interview methods, question design, timing, and communication practices

To ensure the product truly addresses clinical pain points, we conducted in-depth semi-structured interviews with target users. Question design: we prepared semi-open core questions in advance, focusing on interviewees' actual experiences and challenges rather than directly introducing our sensor concept to avoid preconceived bias; questions covered difficulties in daily CKD management, pain points in hospital workflows, and expectations for new monitoring methods; each interview had 2 – 3 core questions plus several follow-ups, chosen flexibly based on the conversation. Process & timing: each interview lasted ~30 minutes; introductions and framing were kept within 3 minutes to

leave ample time; at the end, we asked retrospective questions ( “ Do you have any questions for us?” , “ Are you curious about our sensor?” , “ Any new thoughts during our conversation?” ). Communication style & cultural context: in some cases (e.g., non-local caller ID), speaking Mandarin directly could trigger suspicion or lead to call termination, making pre-planned communication strategies crucial. We adapted style to local contexts across China: in rural Sichuan, we used local numbers and had team members who spoke the dialect conduct interviews to avoid scam mislabeling and build rapport; depending on context, we used Mandarin, Sichuanese, Shandong dialect, or Shanghainese.

#### 8.8.4. Validation design (three sequential methods and linkage)

We used three sequential methods—co-created patient journey mapping, contextualized prototype evaluation, and function-card prioritization—to test feasibility and effectiveness and to guide iterative optimization. For each method we specified the rationale, problems addressed, process, results, and linkage so evidence from each step informed the next.

#### 8.8.5. Co-created journey mapping (purpose, implementation, findings)

Purpose: with patients, map the full pathway (screening → diagnosis → routine follow-up → progression → dialysis), integrate fragmented needs into a system view, identify stages needing real-time monitoring and high-impact touchpoints, and direct solution design. Implementation: an online workshop (~2 hours) with a stage-3 CKD patient, a caregiver of a dialysis patient, and a nephrology nurse. Using a shared whiteboard and sticky notes, participants marked key activities, emotions, and pain points. Examples: patient anxiety/inconvenience during follow-up; nurse noted inability to detect deterioration early at emergency visits. Findings: a current-state map and a future journey embedding the sensor. Critical points—Early screening: asymptomatic/low awareness → missed intervention window; need health education + community screening. Routine follow-up (CKD 4): anxiety awaiting monthly labs, no visibility, travel burden → optimal entry for daily at-home creatinine checks with alerts. Acute deterioration: undetected decline → ED/ICU (AKI); detection days earlier could prevent/mitigate.

#### 8.8.6. Scenario-based prototyping (implementation, procedure, findings, improvements, preliminary value)

Goal & method: validate usability and impact in realistic contexts—can patients detect problems earlier, and can clinicians access timely, actionable information more easily? Why CGM: because our continuous creatinine monitor is in development and, per SensUs guidance to simulate key elements with current tech, we used continuous glucose monitoring (CGM) to replicate the wear experience and gather scenario-based feedback. Implementation & participants: Scenario—first week of at-home use by a stage-3 CKD patient. Prototype—low-fidelity app + existing devices. Two CGMs (Yuwell Anytime 4 Pro, SiBionics CGM) were worn at different times by two team members (a designer and an engineer). Period—May – June; each device worn ~2 weeks (full sensor lifecycle). Real-time glucose readings were assumed as creatinine in the scenario; the app showed daily values, trends, and threshold alerts. Scripted events—Day 3: “Creatinine up 15% vs. yesterday—please arrange a follow-up test soon.” Day 7: sustained rise beyond the safety threshold; red alert: “Above safe range—contact your doctor immediately.” Procedure—Stage 1: daily use (wear the sensor—CGM on upper arm simulating a wristband—and check readings/trends). Stage 2: alerts (on Day 3 decide whether to seek confirmatory testing; on Day 7 follow instructions, e.g., call nephrologist). A mock hospital response flow guided the interaction. Findings—Reassurance from continuity: seeing “creatinine” change daily reduced uncertainty and anxiety. Red alert drives action: the urgent sound and red screen prompted an instinctive response; testers said they would contact a doctor or go to the hospital immediately. Versus monthly testing: daily continuous monitoring yielded more timely, continuous reference data, helping clinicians spot abnormal trends earlier and intervene sooner. Areas for improvement—Wear comfort (nighttime foreign-body sensation, concern about shifting/dislodging) suggests our creatinine sensor should be smaller, softer, and optimized for placement. Data management: at scale, uploads could burden clinicians; the backend should add intelligent filtering/aggregation (e.g., threshold/change-rate triggers) and deliver concise trend reports. Preliminary value—in simulation, the Day-7 alert surfaced abnormality ~3 weeks earlier than a once-monthly creatinine test; even if only 10% of early-stage patients seek earlier care, AKI-related hospitalizations could drop. These projections require large-scale clinical validation, but qualitatively support the design direction.

#### 8.8.7. Early-intervention impact sketch (assumptions & caveats)

Comparing to a monthly-test baseline, the Day-7 alert exposes abnormality  $\approx 3$  weeks earlier. If 10% of early-stage patients act on such alerts and present earlier, AKI-related

admissions may fall. This is a scenario-based projection and must be validated with large-sample clinical studies.

#### 8.8.8. Function card sorting (cohorts, full candidate list, findings)

Rationale: prioritize core functions and avoid low-priority investment via user-driven ranking. Implementation & participants: 5 CKD patients + 3 nephrologists sorted 10 candidate features into essential / nice-to-have / not necessary and selected top-3 (clinicians from a clinical-utility lens). Full list (10): (1) Continuous creatinine (real-time + trends); (2) Expanded parameters (e.g., glucose, potassium); (3) Abnormal-threshold alerts; (4) Patient app (trends, guidance); (5) Doctor platform (remote access); (6) Cloud storage + AI analytics; (7) Comfort-focused design (waterproof, sleep-friendly); (8)  $\geq 14$ -day battery life; (9) Cost/insurance compatibility (affordable, reimbursable); (10) Additional features (e.g., AI kidney assistant). Findings: Patients universally marked continuous creatinine and abnormal alerts as essential; 4/5 also prioritized comfort. Clinicians favored expanded parameters (esp. potassium) and doctor platform/cloud analytics. Other notes: battery life = medium priority (weekly charging acceptable); cost/insurance = medium – high priority; glucose tracking/AI assistants lower than core kidney monitoring. Implications: build first what both groups prioritized—continuous creatinine + key electrolytes, timely alerts, and a doctor-facing data platform—while optimizing comfort and integrating with hospital systems; defer secondary features.

#### 8.8.9. Interview content and CKD pain-points (moved from 4.1.2 & 4.1.3)

Interview content (selected reflections): early cases are often misdiagnosed as gout and delayed for economic reasons, pushing progression to advanced stages; a young patient noted that 1 – 2 months earlier detection would likely have improved outcomes and his acute attack progressed to dialysis, underscoring the need for timely monitoring and alerts; a physician stressed: “Creatinine is central to CKD management; from stage 3 onward, track renal decline and dialysis timing,” recommending long-term monitoring and inclusion of electrolytes (e.g., potassium, calcium) to flag complications (e.g., hyperkalemia), since creatinine alone is insufficient for risk assessment.

CKD pain-points & needs: Low early screening & delays—adult CKD prevalence  $\approx 10.8\%$  (>100M patients), awareness  $\approx 12.5\%$ ; as a “silent killer,” CKD is often missed until late; early symptoms are ignored or misdiagnosed (e.g., gout), wasting the optimal intervention window → need more accessible early monitoring. Infrequent,

discontinuous data—early/mid-stage patients typically test monthly or quarterly; travel and cost reduce adherence, especially in remote areas; without continuous out-of-hospital monitoring, renal decline can accelerate between visits, raising AKI risk. Patient burden & anxiety—frequent blood draws are “troublesome and nerve-racking” ; some reduce testing due to costs; waiting for results fuels anxiety and regret when deterioration is found late → patients need real-time visibility to reduce uncertainty and stress. Clinician needs—from stage 3, decline often accelerates; sporadic outpatient labs are inadequate; clinicians want continuous, physiologic-condition creatinine trends plus key electrolytes (e.g., potassium) to catch dangers like hyperkalemia early, with data integrated into hospital systems and ideally paired with clinical expertise/AI to improve alert accuracy and embed into decisions. Cost & integration—patients want affordable or reimbursable devices; rural/grassroots willingness to pay is limited; alignment with chronic-disease outpatient reimbursement would aid adoption; devices should be hygienic and easy to use (e.g., replaceable/recyclable components to prevent cross-infection) to boost long-term acceptance and sustainability.